Development and validation of a smartphone-sized device for cardiac monitoring using four precordial electrodes

Nynke M. de Vries

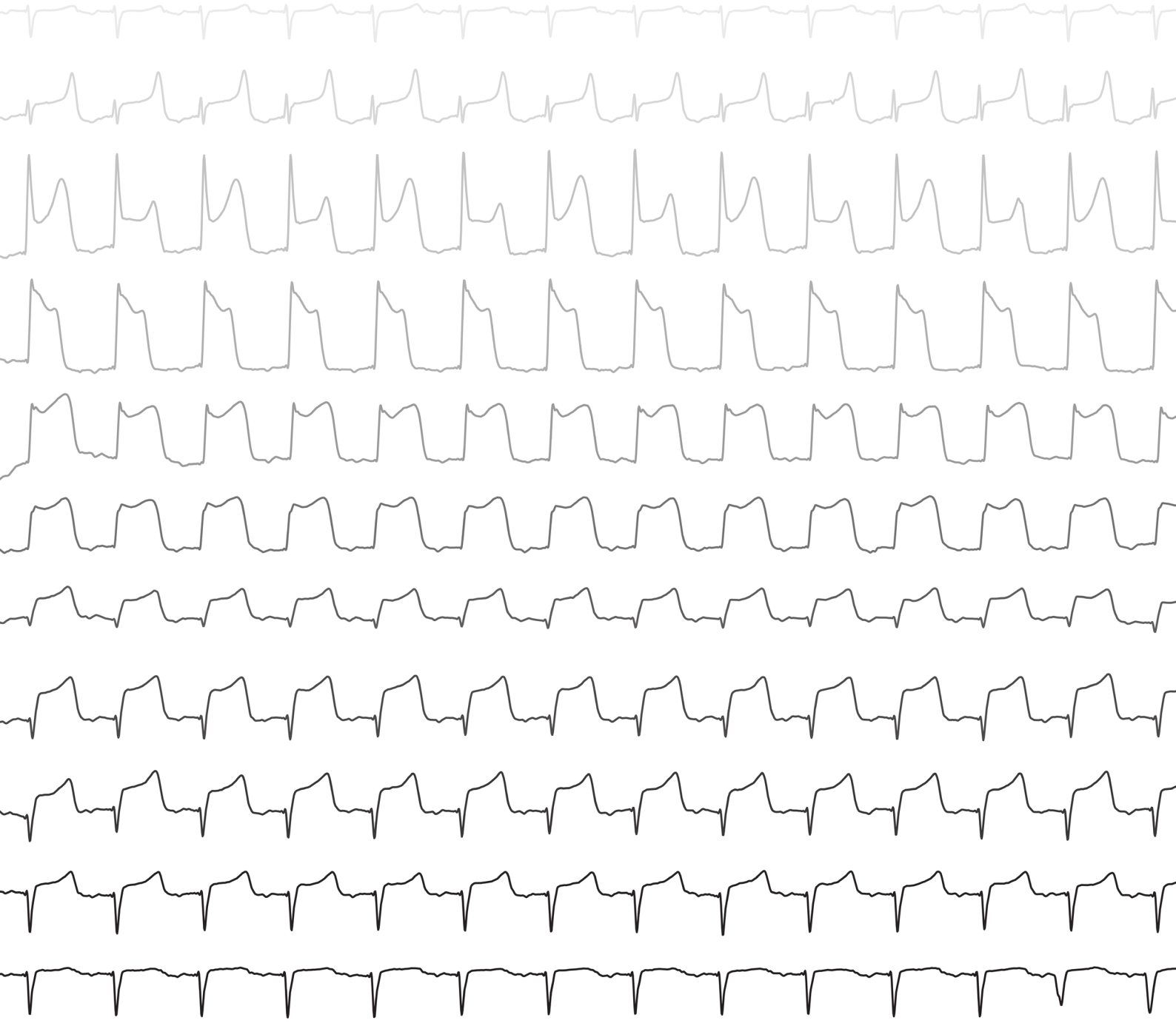

Development and clinical validation of a smartphone-sized device for cardiac monitoring using four precordial electrodes

Master thesis

Nynke M. de Vries

Publication: April 14th 2022
Colloquium: April 25th 2022

Educational institution:
University of Twente, Enschede, the Netherlands
Techmed Centre/Faculty of Science & Technology
Master Technical Medicine, track Medical Imaging & Interventions

Clinical internship institution:
University Medical Center Utrecht
Department of Cardiology

Graduation committee:
Chair & Technical supervisor
Prof. dr. ir. Cornelis H. Slump
Faculty of Electrical Engineering, Mathematics and Computer Science (EEMCS), Robotics and Mechatronics (RAM), Enschede, The Netherlands

Technical supervisor
Dr. René van Es
University Medical Center Utrecht, Department of Cardiology, Utrecht, The Netherlands

Clinical supervisor
Dr. Rutger J. Hassink MD
University Medical Center Utrecht, Department of Cardiology, Utrecht, The Netherlands

Process supervisor
Drs. Paul A. van Katwijk
Faculty of Science and Technology (TNW), Technical Medicine, University of Twente, Enschede, The Netherlands

External member
Drs. Rob S.P. Warnaar
Faculty of Science and Technology (TNW), Cardiovascular and Respiratory Physiology (CRPH), Enschede, The Netherlands

Abstract

Introduction The electrocardiogram (ECG) is one of the most important diagnostic tools in medicine, with an estimated 300 million ECGs recorded each year worldwide[1]. In the UMC Utrecht, a mobile device for ECG acquisition (miniECG) was developed that uses four precordial electrodes to obtain a multi-lead ECG. The miniECG was designed to bring 12-lead ECG diagnostic accuracy to the patient home. The goal of this research was firstly to investigate the detection of cardiac ischemia using the miniECG and secondly to gain insight into the differences and similarities of the miniECG and 12-lead ECG.

Methods This thesis incorporates three studies. An animal study was performed, in which MiniECG and 12-lead ECG recordings were acquired simultaneously before, during and after coronary artery occlusion and ST-deviation (ST-elevation and ST-depression) was evaluated. A clinical pilot study was performed in the Meander Medical Centre (MMC) and University Medical Center Utrecht (UMC Utrecht) to evaluate presence of ST-deviation in patients with cardiac ischemia. Patients with chest pain presenting at the Emergency Room (ER) received both a miniECG and 12-lead ECG. Prescence of ST-deviation was evaluated by two independent cardiologists. Lastly, a clinical study was set-up to evaluate detection of the full spectrum of ECG abnormalities by the miniECG. Preliminary analysis of this study focused on an investigation of normal sinus rhythm criteria for the miniECG and criteria for the detection of common ECG abnormalities.

Results MiniECGs showed early and large ST-deviation compared to 12-lead ECG during 75 minutes of porcine coronary artery occlusion. ST-deviation in the animal model peaked around 10 and 30 minutes, respectively, after which ST-deviation decreased. MiniECG ST-deviation was observed by two cardiologists in 48% of ST-elevation Myocardial Infarction (STEMI) patients. Detection of miniECG ST-deviation was related with TIMI-flow and ST-deviation at hospital arrival was more often confirmed in a 12-lead ECG or 1-lead monitoring ECG in patients with miniECG ST-deviation. Draft criteria for normal SR were established.

Conclusion The studies show the potential of the miniECG in the detection cardiac abnormalities. More research into factors influencing miniECG ST-deviation is needed before the added value of the miniECG in the early detection of cardiac ischemia can be established. In future research, time between miniECG and 12-lead reference ECGs should be minimized to mitigate the dynamic nature of ECG changes as a factor in the capture of these abnormalities.

List of abbreviations

AC	Alternating current
AF	Atrial fibrillation
AI	Artificial intelligence
AMI	Acute myocardial infarction
ANOVA	Analysis of variance
AP	Angina pectoris
CAG	Coronary angiography
CIE	Computerized interpretation of the ECG
DL	Deep learning
ECG	Electrocardiogram
ER	Emergency room
GE	General Electric
IPL	Infero-posterolateral
i.v.	Intravenous
i.m.	Intramuscular
IQR	Interquartile range
LA	Left arm
LAFB	Left anterior fascicular block
LAD	Left anterior descending coronary artery
LBBB	Left bundle branch block
LL	Left leg
LVH	Left ventricular hypertrophy
MMC	Meander Medical Centre
NSTEMI	Non-ST-elevation myocardial infarction
PAC	Premature atrial complex
PCI	Percutaneous coronary intervention
PPV	Positive predictive value
PVC	Premature ventricular complex
RA	Right arm
RBBB	Right bundle branch block
RL	Right leg
STEMI	ST-elevation myocardial infarction
TIMI	Thrombolysis in Myocardial Infarction
UMCU	University Medical Center Utrecht
VF	Ventricular fibrillation
VT	Ventricular tachycardia

Contents

1 General introduction

The electrocardiogram (ECG) is one of the most important diagnostic tools in medicine, with an estimated 300 million ECGs recorded each year worldwide[1]. The current clinical standard 12-lead ECG uses four limb electrodes and six precordial electrodes to map the electrical activity of the heart (**Fig. 1.1**). Interpretation of the ECG is a specialized task, incorporating knowledge on anatomy, electrophysiology, and pathophysiology, with visual pattern recognition and diagnostic reasoning[2].

Limited availability of ECG

The life-threatening nature of acute cardiac disorders requires rapid acquisition and interpretation of the ECG in emergency medical settings[3]. For patients suffering myocardial ischemia, pre-hospital ECG acquisition has shown to significantly decrease time-to-treatment, leading to lower mortality and less severe chronic disease[4–7].

Availability of 12-lead ECG is currently limited to specific locations, such as the hospital, some general practitioners' offices and some nursing homes. Even where ECG devices are available, these might have to be retrieved from central locations, taking valuable time. Elsewhere, patients with cardiac symptoms depend on the arrival of an ambulance or referral to hospitals for assessment of the ECG. These limitations on ECG availability can cause diagnostic delays, leading to higher mortality and morbidity of cardiac disease[8–10].

In addition, availability of 12-lead ECG is bounded by the need for trained healthcare professionals regarding interpretation of the ECG. Studies show inferior accuracy of non-cardiologist physicians and computer interpretation compared to cardiologists [2,11–14]. While modern infrastructure enables remote interpretation of the ECG by cardiologists, this poses a high burden on cardiologists and results in high healthcare costs. Inaccurate ECG interpretation the other hand causes false-positive interpretations resulting in unnecessary medication use and unnecessary additional diagnostics[15,16].

Benefits of the miniECG

The healthcare system can benefit from mobile ECG devices, meaning easily accessible for a patient at any time and easy to operate without the need for a healthcare professional, to be used to detect the full spectrum of cardiac abnormalities. In the UMC Utrecht, a mobile device for ECG acquisition (miniECG) that uses four precordial electrodes to obtain a multi-lead ECG was developed (**Fig. 1.2**). The device is portable

and reusable as it incorporates sustainable dry electrodes instead of disposable gel electrodes. The miniECG can be operated using a mobile app, which after short instructions can be used without the need for any additional professional equipment. The current prototype of the device, miniECG 1.1, is suitable for clinical research. Healthcare professionals can use the device after short instruction, with incidental support of the research team. For the miniECG 2.0, patients should be able to record and sent an ECG using the miniECG app, without any assistance outside of the app's instructions.

Similarities of the miniECG and 12-lead ECG

The 12-lead ECG uses both limb and precordial electrodes to obtain the ECG. The six extremity leads of the 12-lead ECG are measured or calculated using the four limb electrodes (**Fig. 1.1**)[17,18]. Lead I measures the potential-difference between the right arm (RA) and left arm (LA) electrodes and lead II measures the potential-difference between the left arm (LA) and left leg (LL) electrodes. Lead III and the augmented leads (aVR, aVL, aVF) are combinations of leads I and II (**Fig. 1.1**). The right leg (RL) electrode is not reflected in any of the 12-leads. This electrode functions to reduce alternating current (AC) common-mode noise that couples into the body[19]. Precordial leads are measured using the precordial electrodes in reference to Wilson's Central Terminal (WCT). The WCT is derived by averaging of the right arm, left arm and left leg signal, which is assumed to be steady and with negligible amplitude during the complete cardiac cycle[18,20].

The miniECG uses only four precordial electrodes to record 8 independent leads (**Fig. 1.2**). Precordial leads comparable to 12-lead V1, V2 and V3 are measured using three of the precordial electrodes of the miniECG in reference to the other three electrodes. Lead M3 is an additional lead, using the fourth electrode of the miniECG and remaining three electrodes as a reference. No such right sided precordial lead is measured in the 12-lead ECG (**Fig. 1.1**). The standard 12-lead ECG is sampled at 500Hz and filtered to a bandwidth of 0.05-150Hz. The current version of the miniECG records at 250Hz. Filtering is optimized for different studies individually.

Research aim

ST-elevation, the ECG hallmark of cardiac ischemia, is only visible in the leads facing the ischemic zone. Most available devices for cardiac home monitoring have a limited number of leads and are therefore not able to reach the detection levels of the clinical 12-lead ECG[21,22]. To assess the shortcoming of currently available devices, this research focusses firstly on the capture of cardiac ischemia by the miniECG. Secondly, the possibility of detection of the full-spectrum of ECG abnormalities will be explored.

a

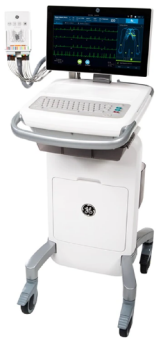

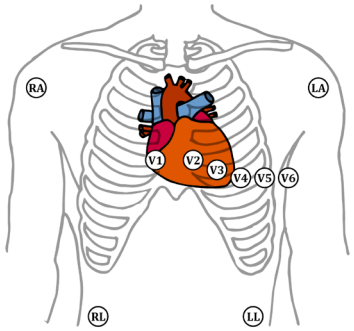

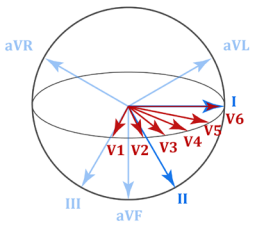

$$III = II - I$$

$$aVL = \frac{(I - III)}{2}$$

$$aVR = -\frac{(I + II)}{2}$$

$$aVF = \frac{(II + III)}{2}$$

b

Surname, Name. **ID:xxxxxxx** **09-MRT-2021 13:36:42** **UMC Utrecht-DEFLT ROUTINE-OPVRAAG**

Date of birth: xx-xx-1994
Sex: Woman
Kamer:

Vent. frequentie	77	bpm
PR-interval	150	ms
QRS-duur	86	ms
QT/QTc	364/411	ms
PRT-assen	68 76	56

SINUSRITME
NORMAAL ECG

Technicus: xxx
Testind: xxx

Onbevestigd

Opmerking:

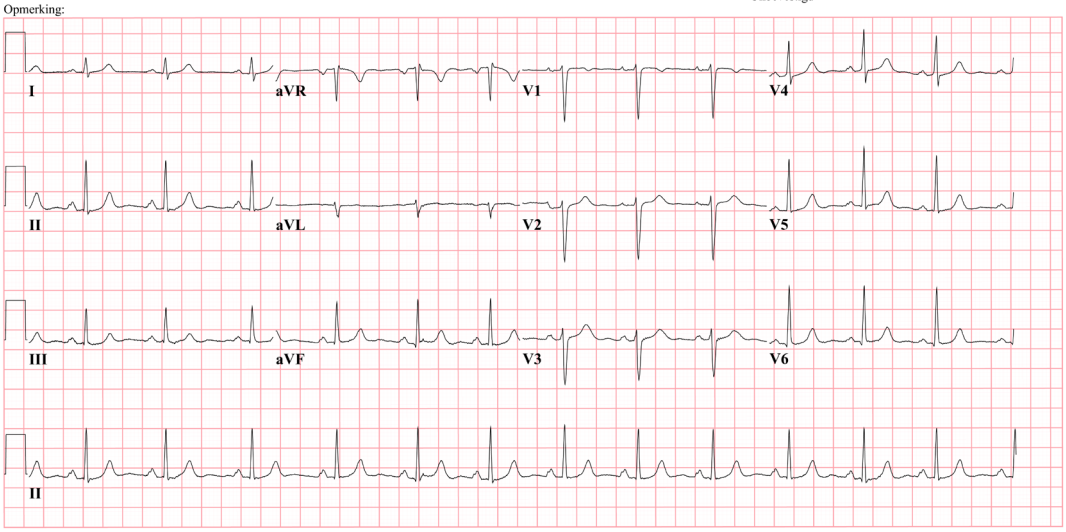

25mm/s 10mm/mV 150Hz 9.0.10 12SL 243 CID: 1

BSN: xxxxxxxxxx

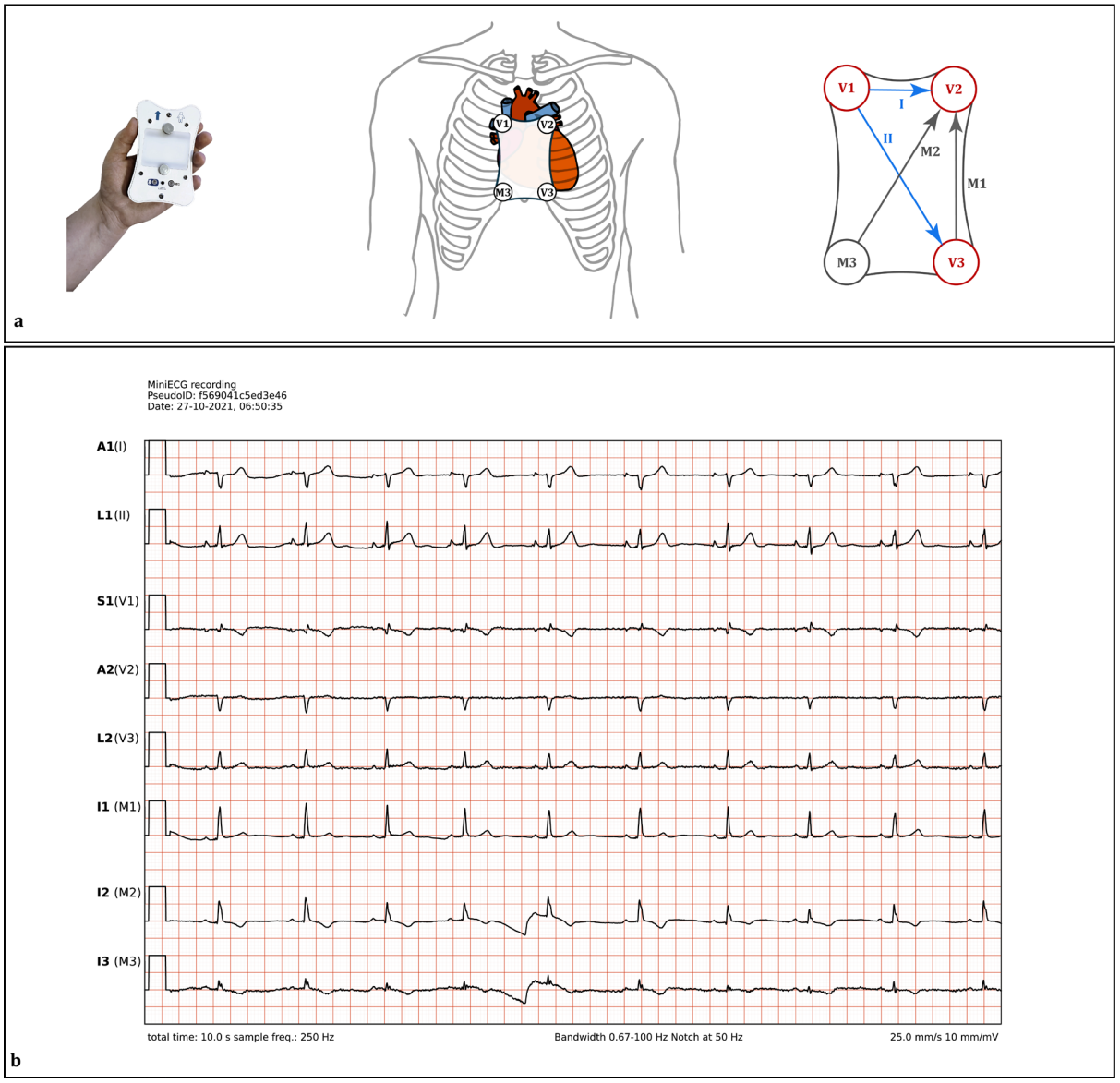

Figure 1.2: a. MiniECG 1.1 (UMC Utrecht) including electrode positioning and corresponding lead configuration. b. Mini ECG recording of a 26-year-old female showing normal sinus rhythm.

2 Thesis outline

This thesis elaborates on three studies evaluating the capture of ECG abnormalities by the miniECG. In ***Chapter 3***, a porcine study on ischemia detection is presented. In this study miniECG and 12-lead ECG were recorded before, during, and after coronary artery occlusion in eight animals. Trends and magnitude of ST-elevation and reciprocal ST-depression were evaluated.

In ***Chapter 4***, a pilot study into the miniECG focusing on ischemia detection is presented. For this study, patients with chest pain received both 12-lead ECG and miniECG. These ECGs were evaluated to assess the accuracy of the miniECG in detection of cardiac ischemia with different locations of infarction.

To be able to use the miniECG to detect the full spectrum of ECG abnormalities, a second clinical study aiming to examine miniECGs and ECGs of >10,000 patients started in November 2021. Preliminary results of this study are discussed in ***Chapter 5***.

In ***Chapter 6,*** implications for miniECG development and validation are discussed and recommendations are provided.

3 Detection of ST-segment changes using a novel mobile ECG device with four precordial electrodes in a porcine coronary artery occlusion model

Introduction

The electrocardiogram (ECG) is a crucial modality in the diagnosis of acute cardiac disease. The life-threatening nature of various cardiac disorders such as myocardial ischemia, requires rapid and accurate ECG interpretation and accordant treatment. For patients suffering myocardial ischemia, pre-hospital ECG acquisition has shown to significantly decrease time-to-treatment, lowering the morbidity and mortality[5–7].

To improve time-to-treatment, the ECG can be acquired in pre-hospital professional settings by the general practitioner or by emergency staff including ambulance nurses, or for example by the patient at home. The latter poses the need for portable and small ECG devices, easily accessible for patients at any time and straightforward to operate without the need for a healthcare professional. Recently, several portable and small ECG devices have been investigated for this purpose[22]. While evidence shows high sensitivities regarding the detection of rhythm disorders, no currently available portable ECG device has yet shown high accuracy in validation regarding detection of cardiac ischemia[21,22].

Recently, we have developed a portable and smartphone-sized device for ECG acquisition with four precordial electrodes to obtain a multi-lead ECG, the miniECG. The device is portable and reusable as it incorporates sustainable dry electrodes instead of disposable gel electrodes or patches. The miniECG is operated using a mobile app, which after short instructions can be used without the need for additional professional equipment or a healthcare professional. This research aims to investigate the ability of the miniECG to capture ischemia induced ST-segment changes during onset, presence and following acute coronary artery occlusion through comparison with 12-lead ECG in a porcine model.

Methods

Animals

Eight female Topigs Norsvin pigs with a median weight of 65.0 kg [IQR 63.0, 66.5], were included in this research. All measurements were performed in addition to an ongoing project under project number (AVD1150020172624) authorized by the Animal Welfare Body in compliance with the Guide for the Care and Use of Laboratory Animals[23].

Anaesthesia protocol

Starting 10 days before the experiment, the animals were given daily doses of clopidogrel (75mg) and amiodarone (800mg, first dose 1200mg). Acetylsalicylic acid (320mg) was administered one day before the experiment. On the day of the experiment, the animals were premedicated with a single dose of ketamine (10mg/kg), midazolam (0.5mg/kg), atropine (0.05mg/kg) and carprofen (2-3mg/kg) i.m.. General anaesthesia was induced with a single dose of thiopental (4mg/kg) i.v. and maintained by continuous i.v. administration of cisatracurium (0.7mg/kg/h), midazolam (0.4mg/kg/h) and sufentanil (2.5μg/kg/h). After induction of general anaesthesia, 300mg of amiodarone was infused during 45 minutes.

The animals were mechanically ventilated with a positive pressure ventilator, using a mix of oxygen and air (FiO_2 0.5), at a respiratory rate of 12/min and a tidal volume of 10 mg/kg. The positive end-expiratory pressure was adjusted between 2-3 cm H_2O to maintain an end-tidal CO_2 pressure between 35 and 45 mmHg. Body temperature was maintained between 36.5°C and 38°C with heating pads.

Heparin (15,000 IE) was given prior to cannulation of the carotid artery, prior to balloon occlusion and prior to reperfusion for anticoagulation. Blood pressure was monitored continuously by an arterial pressure catheter inserted in a peripheral artery.

Occlusion and reperfusion

With the animal in supine position, the carotid artery and jugular vein were cannulated using 8-French sheets. Coronary angiography (CAG) was performed to map the anatomy of the left anterior descending artery (LAD). A 3.0mm balloon catheter (Sapphire II Pro, OrbusNeich, Hong Kong) was positioned after the first or second diagonal branch depending on coronary artery anatomy to induce sufficient ischemia while minimizing the risk of death due to refractory ventricular fibrillation (VF) during the experiment. The balloon catheter was pressurized to 6 bar to induce occlusion, after which successful occlusion was confirmed through CAG. After 75 minutes of occlusion the catheter was removed and reperfusion occurred

during 60 minutes (**Fig. 3.1**). The animals were euthanized after 60 minutes of reperfusion by administration of KCl (1500mg) i.v..

Resuscitation protocol

In case of hemodynamically intolerable arrhythmias, i.e. VF and sustained ventricular tachycardia (VT), 200 joules shocks were applied using the external paddles of a Heartstart XL defibrillator (Phillips, the Netherlands) alternated with manual chest compressions if needed. A dose of amiodarone (150mg) was administered during every episode, with a maximum of three administrations.

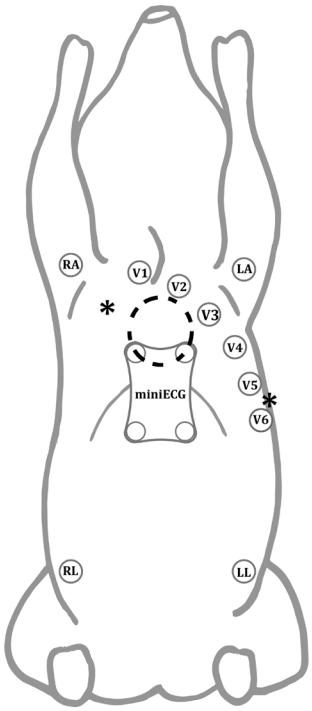

Figure 3.1: Positioning of miniECG and 12-lead ECG electrodes, approximate location of the heart (dashed circle) and positioning of the defibrillation paddles (asterisks).

ECG recordings

For this experiment a prototype version of the miniECG (miniECG 1.0, UMC Utrecht, the Netherlands) was used. The miniECG device uses four precordial stainless-steel electrodes to record eight independent leads, at a sample frequency of 250Hz for 10 seconds (**Fig. 1.2**). Leads I, II, M1 and M2 of the miniECG are measured using electrode pairs. Leads V1, V2, V3 and M3 of the miniECG are measured using the other three electrodes as a reference. Electrode gel (Signa Gel, Parker) was applied to the miniECG electrodes for optimal electrical conduction. To obtain miniECG recordings, the miniECG device was positioned in the

sternal midline of the animals, where the chest wall is flat to ensure skin contact of all 4 electrodes (**Fig. 3.1**). 12-lead ECG electrodes were positioned according to standard clinical care, whilst keeping the central chest free for the miniECG and defibrillation (**Fig. 3.1**).

For each animal, three 10-second baseline miniECG recordings were acquired 5 minutes before occlusion. During occlusion, recordings were performed at interval of 1 minute for the first 10 minutes of occlusion and at an interval of 5 minutes for the rest of the experiment (**Fig. 3.2**). Recordings were only performed if did this not interfere with essential steps of the rest of the experimental protocol, such as the administration of defibrillation shocks. MiniECG recordings were filtered bidirectionally using a digital 3th order bandpass Butterworth filter with cut-off frequencies of 0.67Hz and 40Hz respectively. For comparison, 12-lead ECG recordings, sampled at 1200Hz and filtered to a bandwidth of 0.05 to 1200 Hz were acquired using the Cardioperfect PRO ECG Recorder (Welch Allyn, USA).

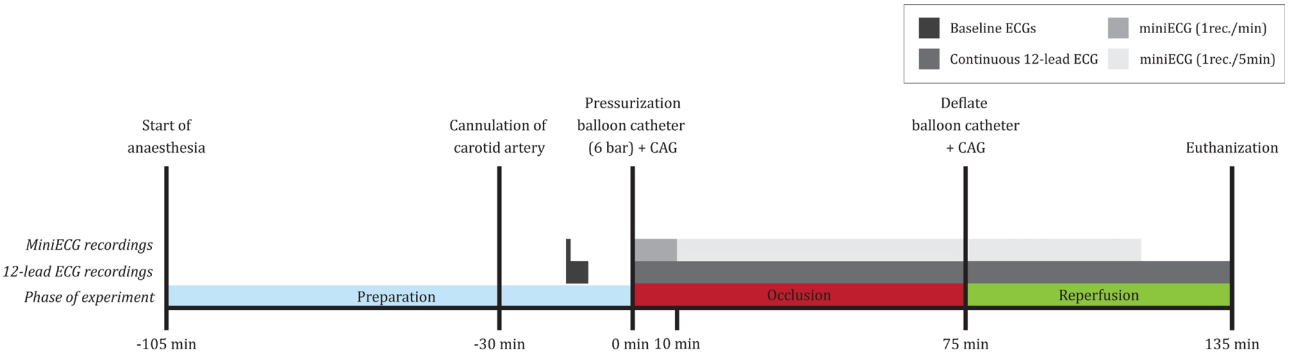

Figure 3.2: Overview of experimental protocol.

Assessment of ECGs

ST-deviation, defined as ST-elevation or reciprocal ST-depression, was measured at the J-point[24]. This was done for all leads of all miniECG recordings and at corresponding timepoints on the 12-lead ECGs. Measurements within 5 minutes after defibrillation shocks were excluded from analysis. Baseline QRS-amplitude (R-S) and T-wave amplitude were measured for both the miniECG and 12-lead ECG before occlusion.

Statistical analysis

Median and interquartile ranges (IQR (Q1, Q3)) were calculated for the baseline characteristics. For each animal, the miniECG lead and 12-Lead ECG lead showing the largest ST-deviation were identified. For these leads, ST-deviation trendlines were fitted using MATLAB's (The Math Works, Inc. MATLAB. Version R2020b) smoothing spline fit for the occlusion period and reperfusion period separately. The smoothing

parameter p was set to 0.05 to minimize noise in the trendlines. Weights w_i were set to 1, except for the pre-occlusion baseline measurement ($w_1 = 10$) to ensure the curve to fit this baseline ST-deviation value. Mean and 95% confidence interval (CI) of ST-deviation were evaluated using the trendlines for the miniECG and the 12-lead ECG separately. Paired T-tests were used to assess differences between the miniECG and 12-lead ECG, regarding QRS amplitude at baseline and ST-deviation at peak ST-deviation at set timepoints.

Results

All eight animals survived the occlusion and reperfusion periods, despite frequent ventricular arrhythmias. During the occlusion period, the animals received a median of 22 [Q1-Q3 8-36] defibrillation shocks for arrhythmias (**Table 3.1**). Angiography showed complete occlusion of the LAD after inflation of the balloon catheter in all animals (**Fig 3.3**) and return of the blood flow after deflation of the balloon catheter.

Table 3.1: Animal characteristics

	Animal								
	1	**2**	**3**	**4**	**5**	**6**	**7**	**8**	**Median (IQR)**
Demographics									
Weight (kg)	67.0	66.0	67.5	66.5	64.0	63.5	57.0	60.5	65.0 (63.0, 66.5)
Events									
Episodes of hemodynamically intolerable arrhythmia during occlusion	3	0	9	3	7	3	2	2	3 (2, 4)
Defibrillation shocks	9	0	30	75	54	25	6	18	22 (8, 36)
Time to first defibrillation shock (minutes)	18.0	-	4.6	4.0	16.5	17.6	16.7	15.5	16.5 (10.1, 17.2)
Chest compression sessions	0	0	0	3	3	2	0	1	1(0, 2)
Amiodarone administered during experiment (mg)	450	0	450	450	450	450	300	300	450(300, 450)
Dopamine administered IV (start time in minutes)	-	-	30	32	38	32	-	-	32(31.5, 33.5)

In 98% of miniECG recordings, no disturbing baseline wander or high frequency noise was observed and accurate assessment of morphology of the ST-segments was possible. In 2 animals no miniECG recordings were acquired in the first 30 minutes of occlusion due to technical failure. Apart from this, miniECG recordings could most often be performed at pre-specified timepoints (**Supplement S3.1**). In animal 4 the 12-lead ECG recordings failed between 20 and 45 minutes of occlusion due to technical failure.

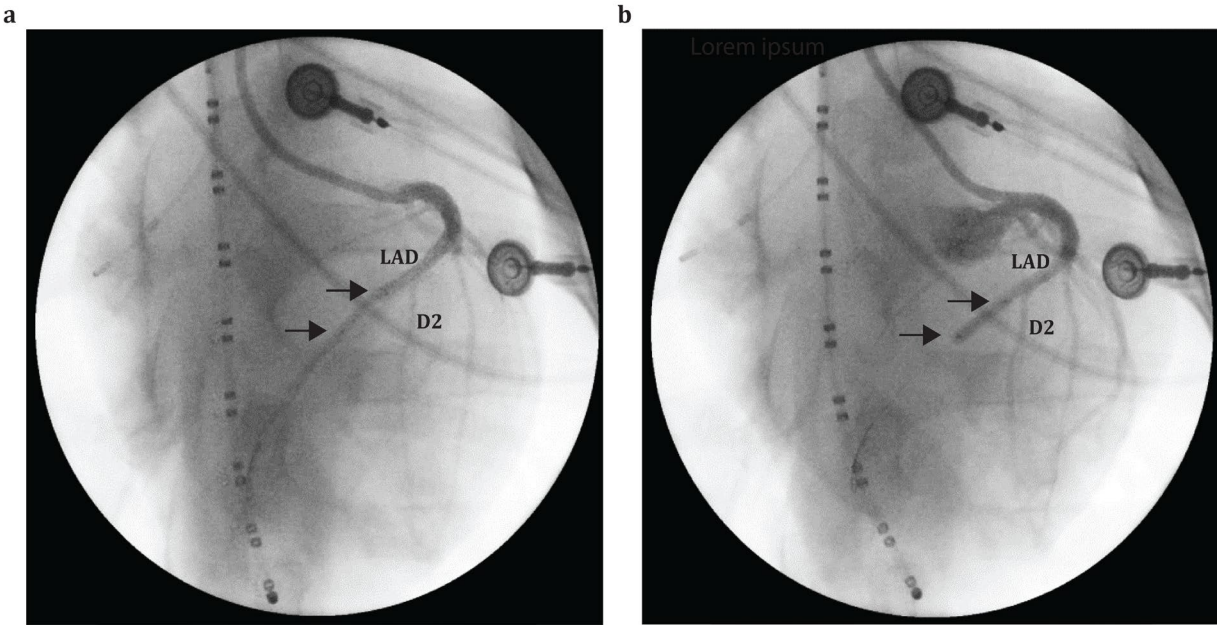

Figure 3.3: a. Angiogram of animal 8 with balloon catheter (arrows) positioned after the second diagonal branch of the LAD (D2). b. After inflation of the balloon catheter blood flow to the distal LAD is restricted.

Difference in ST-deviation

At baseline before occlusion, ST-deviation was <0.5mm for all animals. Both the miniECG and 12-lead ECGs showed ST-deviation of large magnitude from the early occlusion period onwards (**Fig. 3.4, 3.5**). The mean magnitude of the miniECG ST-deviation was larger compared to 12-lead ECG ST-deviation during the complete occlusion period, with a small overlap of the 95% CI (**Fig. 3.5**). At 5 minutes of occlusion, mean ST-deviation magnitude was significantly larger with 9.0mm [95%CI 6.0-12.0mm] for the miniECG compared to 2.5mm [95%CI 1.5-3.5mm] for the 12-lead ECG (p=0.004).

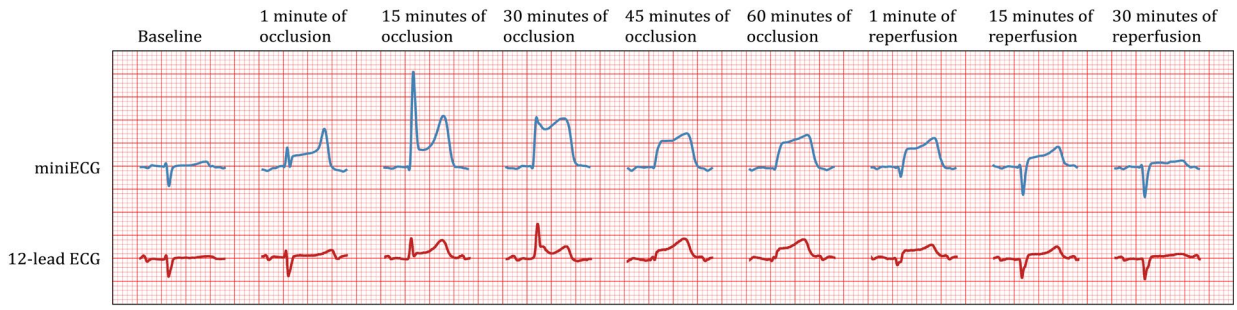

Figure 3.4: Changes in ST-segment at 15-minute intervals during occlusion and reperfusion periods in leads selected based on similar morphology (miniECG lead -II and 12-lead ECG lead V1 in animal 8).

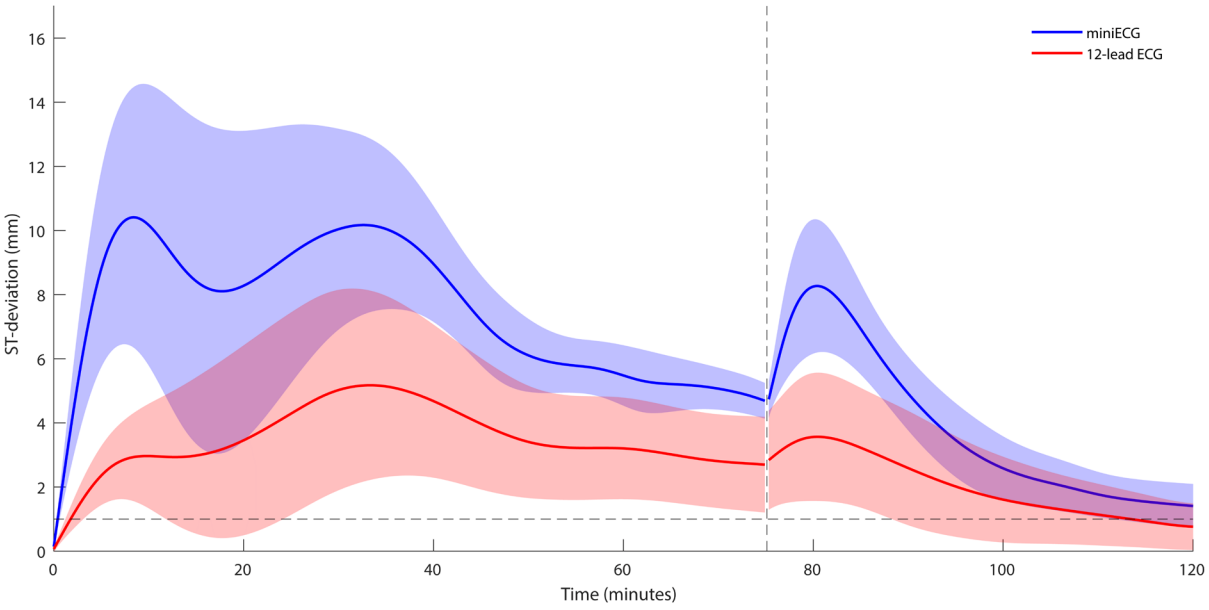

Figure 3.5: Mean ST-deviation and 95%CI of the most deviated leads of the miniECG and 12-lead ECG during the occlusion period and reperfusion period. The horizontal dashed line shows a 1mm threshold for ST-deviation. The vertical dashed line indicates the start of the reperfusion period at 75 minutes.

The difference in ST-deviation between miniECG and 12-lead ECG shows variation between animals. For the first and third animal, the magnitude of ST-deviation on the miniECG and 12-lead ECG was comparable (**Supplement S3.2**). For all other animals, the magnitude of ST-deviation was significantly larger on the miniECG compared to 12-lead ECG. Animal 2 showed the smallest 12-lead ECG ST-deviation during the occlusion. For this animal, ST-deviation was ≤2mm on all 12-lead recordings during the occlusion, and from 15 minutes of occlusion until the start of the reperfusion period no ST-deviation was observed at all. In contrast, all miniECGs recorded in this animal during occlusion showed ST-deviation >2mm.

Correction for baseline T-wave amplitude increased the difference between miniECG ST-deviation and 12-lead ECG ST-deviation (**Supplement S3.3**). After correction of ST-deviation magnitude for baseline QRS-amplitude, the overlap of the 95% CI increased from 15 minutes onwards. For the first 15 minutes, miniECG ST-deviation was still higher compared to 12-lead ECG, without any overlap of the 95% CI.

Leads showing maximal ST-deviation

Maximal ST-deviation was observed in leads II (62.5%), M2 (25%) and I (12.5%) for the miniECG and in leads V3 (37.5%), V4 (37.5%) and V2 (25%) for the 12 lead-ECG. The difference in baseline QRS-amplitude and T-wave amplitude between miniECG and 12-lead ECG were not statistically significant in these leads (p=0.61, p=0.17, respectively) (**Table 3.2**).

Table 3.2: QRS- and T-wave amplitudes at baseline before occlusion

		Animal								
		1	**2**	**3**	**4**	**5**	**6**	**7**	**8**	**Mean [95% CI]**
Leads showing maximal ST-deviation	**miniECG**	M2	II	M2	II	I	II	II	II	-
	12-lead ECG	V4	V3	V4	V3	V4	V2	V3	V2	-
QRS-amplitude (mV)	**miniECG**	0.83	0.87	2.05	0.95	0.51	0.76	0.62	0.53	0.89 [-0.02-1.80]
	12-lead ECG	0.53	0.73	0.91	0.31	0.89	0.87	1.03	0.99	0.78 [0.33-1.24]
T-wave amplitude (mV)	**miniECG**	0.26	0.13	0.25	0.18	0.11	0.17	0.09	0.12	0.16 [0.05-0.28]
	12-lead ECG	0.23	0.09	0.20	0.13	0.40	0.33	0.26	0.20	0.23 [0.05-0.41]

Time of onset of ST-deviation

Recordings were not available for all animals in the first minutes of the experiment, due to technical failure of the 12-lead ECG or miniECG. At one minute of occlusion in four animals both the 12-lead recording and miniECG recording were successful. In three of these animals ST-deviation ≥1mm was observed on the miniECG, compared to one animal with ST-deviation ≥1mm on the 12-lead ECG. At the timepoint of 2 minutes after occlusion, a miniECG and a 12-lead ECG recording were available in five animals, where all five showed ST-deviation ≥1mm on the miniECG versus three on the 12-lead ECG. At the timepoint of 5 minutes of occlusion, ST-deviation ≥1mm was visible for all miniECG and 12-lead ECG recordings in five animals with available data at that timepoint.

ST-deviation peaks

While maximum ST-deviation differs, miniECG and 12-lead ST-deviation showed similar trends during occlusion and reperfusion (**Fig. 3.5**). In general, two peaks in ST-deviation were observed during occlusion. For the miniECG these peaks are more prominent, with local maxima of 10.5mm [95%CI 6.5-14.5mm] at 8 minutes of occlusion and 10.0mm [95%CI 7.0-13.0mm] at 33 minutes of occlusion. For the 12-lead ECG these local maxima are 3mm [95%CI 1.5-4.5mm] at 10 minutes of occlusion and 5.0mm [95%CI 2.0-8.0mm] at 33 minutes of occlusion. After the second peak, ST-deviation decreases for both the miniECG and 12-lead ECG. During reperfusion, a sudden increase of ST-deviation was observed, miniECG and 12-lead ECGs reached maximum ST-deviation of 8.0mm [95%CI 6.0-10.0mm] and 3.5 [95%CI 1.5-5.5mm], respectively, after 5 minutes of reperfusion, after which ST-deviation decreased. In the 40 minutes after reperfusion, ST-deviation did not yet reach baseline values.

Discussion

In this study, we have investigated the ability of the miniECG to capture ischemia induced ST-segment changes during onset, presence and following coronary artery occlusion through comparison with the standard 12-lead ECG in a porcine model of myocardial infarction. This animal model and the controlled setting of this experiment allowed unique evaluation of ST-deviation in relation to the duration of complete coronary artery occlusion.

Difference in ST-deviation

During the complete occlusion and reperfusion periods, the miniECG shows ST-deviation of larger magnitude compared to 12-lead ECG, suggesting higher sensitivity of the miniECG in the detection of cardiac ischemia. This is important as this is the first proof of concept of the miniECG regarding ischemia detection.

Two major mechanisms are considered to underlie ST-deviation in ischemia. Firstly, localized shortening of action potential duration generates currents only during the ST-segment, resulting in primary ST-deviation. Secondly, a localized decrease in resting membrane potential of the ischemic ventricular tissue creates a steady injury current. This current is interrupted during the ST-segment when all cells are depolarized, and is therefore only visible in the ECG in the TQ-segment. As ECG filtering removes the DC offset, the TQ-baseline shift caused by the injury current, results in ST-deviation of the opposite direction[25–27]. The observed magnitude of ST-deviation in specific leads can be explained by the solid angle theory; as a direct consequence of electrode position with respect to the ischemic currents. On top of this, the tissue between the heart and electrodes is not homogeneous, resulting in variable conductivities, thereby also affecting observed ECG amplitudes. This can be clearly observed in body surface potential maps wherein local maxima and minima in ST-deviation appear[28].

As measured ST deviations are strongly influenced by electrode position with respect to the ischemic area, a likely explanation for the relatively smaller magnitude of the 12-lead ST deviation is the craniolateral placement of the precordial 12-lead electrodes [28,29]. This is both further away from the heart, and at a non-perpendicular angle in respect to the antero-septal ischemia of the porcine heart. The miniECG was positioned close to the apex of the porcine heart that is located frontally in the porcine chest and thus close to the ischemic area.

By correcting for baseline QRS-amplitude and T-wave amplitude (**Supplement S3.3)**, placement of the ECG electrodes with respect to the heart was eliminated as a factor in the magnitude of ST-deviation.

The correction for baseline QRS-amplitude decreased the difference between miniECG ST-deviation and 12-lead ECG ST-deviation. However, interestingly, after correction the difference between miniECG ST-deviation and 12-lead ST-deviation for the first 15 minutes remained significant. Thus specifically, this observed phenomenon is most likely to be caused by the electrode placement with respect to the ischemic area instead to the complete heart. Another possible explanation of the differences in ST-segment deviation between the miniECG and 12-lead ECG is the difference in the reference to which the precordial leads are measured. The 12-lead ECG uses Wilson's Central Terminal (WCT) as a reference for the precordial leads, computed by taking the mean of the right arm, left arm and left leg electrodes[18,20]. The WCT is a position at the centre of Einthoven's triangle and thus at the centre of the heart. For the miniECG, all electrodes are placed precordially, and from these electrodes an alternative WCT is constructed by taking the average of the precordial electrodes. As a consequence, all leads are based on different combinations of these precordial electrodes. During coronary artery occlusion, especially of the LAD, potential maps of the body surface show large potential differences of the ST-segment around the left frontal side of the chest in humans[28]. In the porcine heart, with a more frontally oriented cardiac apex, it is expected that the largest potential differences of the ST-segment are observed at the central chest, where the miniECG was placed during this experiment, thereby also explaining the large differences in ST-segment deviation between the 12-lead and miniECG recordings.

Leads showing maximal ST-deviation

Interestingly, the miniECG leads that most often show maximal deviation (II and M2), are measured using the electrodes on the opposite corners of the miniECG. While differences in electrode distance are relatively small in the miniECG, the distance between the electrodes of these two leads is the largest with 10.3cm vs 9cm vertically or 5cm horizontally (**Fig. 1.2**). A possible explanation of the large ST-deviation magnitudes for leads II and M2 could be the fact that the miniECG was positioned partially below the diaphragm (**Fig. 3.1**). This way, the leads of the miniECG are directed not truly in the frontal plane, but slightly oblique towards the transversal plane. In this oblique plane, miniECG records the ECG near the apex of the porcine heart, explaining similarity in the large ST-deviations in leads II and M2.

Time of onset of ST-deviation

The measuring interval of 1 minute and missing data resulted in lack of temporal resolution especially during the first 3 minutes of occlusion where ST-deviation reached ≥1mm for most animals. For this reason,

time of ST-deviation ≥1mm could not be determined with high precision based on the acquired data. Still, it can be concluded that earlier detection of ST-deviation was possible using the miniECG compared to the 12-lead ECG. The difference between one out of four animals showing 12-lead ECG ST-deviation ≥1mm at one minute of occlusion, versus three out of four animals for the miniECG is highly relevant. Evaluation of miniECG and 12-lead ECG ST-deviation at two and three minutes allowed the inclusion of more animals into this sub analysis and results of this affirming the conclusion of earlier detection by the miniECG. The results suggest that the miniECG is able to capture changes in the ST-segment within 1 minute after acute coronary occlusion in a porcine model of transmural anterior infarction.

ST-deviation peaks

Our results show two ST-deviation peaks between 10 and 40 minutes of occlusion after which ST-deviation decreases (**Fig. 3.5**). During reperfusion a short-lived increase in ST-deviation was observed after which the ST-segments normalized. Figueras et al. showed ST-deviation trends of epicardial and endocardial ECG in a 4-hour coronary artery occlusion porcine model[30]. Their data also reveal two distinct ST-deviation peaks between 10 and 40 minutes of occlusion and gradually decreasing ST-deviation after the second peak, similar to our findings[30]. Our findings are in line with those of Kleinbongard et al., who showed larger ST-deviation at 5 minutes of occlusion compared to 55 minutes of occlusion in an animal study on ischemic conditioning[31].

To the best of our knowledge, there have been no publications on the mechanisms behind the two separate peaks in ST-deviation during the first hour of coronary artery occlusion. Interestingly, the timepoints of the observed peaks correlate with incidence and different mechanisms of VF occurrence during coronary artery occlusion as reported in a review by Diego et al[32]. They describe phase 1A arrhythmias occur between 2 and 10 minutes of coronary occlusion and phase 1B arrhythmias between 15 and 30 minutes in porcine and canine models for cardiac ischemia. During phase 1A, bursts of VT occur that most often do not induce VF. Re-entry is suggested to be the primary mechanism of the arrhythmias occurring in this phase. During phase 1B, arrhythmias are suggested to emerge from both focal as well as non-focal sources. Two different mechanisms for the occurrence of VF at the peaks of ST-deviation might be indicative of two different mechanisms for the development of ST-deviation at these peaks. More research is needed to investigate a possible relation between the incidence and mechanisms of VF and peaks in ST-deviation during coronary artery occlusion.

The short-term increase of ST-deviation during reperfusion is most likely caused by reperfusion injury of the myocardium[33–36]. Examples of processes causing reperfusion injury are increased cellular calcium, processes of oxidative stress, rapid restoration of pH and inflammation. Besides, mechanical factors, play a role. Haemorrhage from small vessels that are injured by ischemia but are reperfusable at the time of reflow, leads to an increase of interstitial pressure, which negatively affects perfusion. The occurrence of a reperfusion peak is indicative of a larger final infarction size[37,38].

Effect of defibrillation shocks

The need for defibrillation shocks in case of hemodynamically intolerable ventricular arrhythmias has influenced the study data in two ways. Firstly, during episodes of hemodynamically intolerable ventricular arrhythmias, no miniECG recordings could be obtained, leading to data loss. Secondly, defibrillation shocks have a short-lived effect on the ST-segment, documented to occur shorter than 5 minutes in most cases[39–42]. Defibrillation shocks can cause increase of ST-deviation or temporary transition of ST-elevation into ST-depression[39–42]. The magnitude of ST-deviation is therefore not only influenced by ischemia in this experiment but by these shocks as well. To correct for this defibrillation shock-induced ST-deviation, measurements within 5 minutes after defibrillation shocks were excluded from the analysis. As shocks were administered mostly between 10 and 40 minutes of occlusion, where ischemic ST-deviation increases as well, it is not known whether this completely excludes the effect of the shocks.

Study limitations

A porcine model was used as it resembles the human heart as close as possible, especially regarding coronary anatomy. Nonetheless, the positioning of the porcine heart in relation to the chest is different compared to humans, as well as the anatomy of the conduction system and electrophysiological properties[43,44], resulting in an abnormal ECG considering clinical conventions. Therefore, results of this study cannot be directly translated into human clinical setting.

The measuring interval of 1 minute and missing data resulted in lack of temporal resolution especially during the first 3 minutes of occlusion where ST-deviation reached ≥1mm for most animals. For this reason, time of ST-deviation ≥1mm could not be evaluated for all animals, lowering the power of this analysis. The rapid increase of ST-deviation on the miniECG in the first minutes, was not expected based on experience of the research team with 12-lead ECG recordings during occlusion in porcine experiments, that showed only small ST-deviation. The used prototype version of the miniECG was not optimized for

recording more often than one 10s recording every minute and for this reason the measuring protocol could not be adapted during the experiments.

The number of animals included in this study is low considering the high inter-subject variability of ST-deviation for both miniECG and 12-lead ECG. Therefore, more research is needed to confirm our findings.

Future perspective

Time delay between onset of symptoms and seeking medical attention is a major factor in mortality and morbidity in patients with acute myocardial infarction (AMI)[45]. The miniECG was developed as a portable, smartphone sized ECG device for easy self-use by patients, enabling the acquisition of an ECG within one minute. With future incorporation of algorithms for automated miniECG analysis, this may bring the diagnostic capabilities of the ECG to the patient's home. The miniECG may decrease time delay between onset of symptoms and seeking medical attention, as it gives patients an accessible tool to acquire an ECG themselves. When ischemia is detected early using the miniECG, this could decrease mortality and morbidity of AMI, as hospitals can be alerted and can respond and prepare accordant treatment[46–50].

On the other hand, home-based electrocardiography has the potential to increase quality of life by reassuring patients when the miniECG shows no ischemic ECG changes. For patients with paroxysmal atrial fibrillation, home-monitoring using portable ECG tools has shown to increase quality of life even decreasing the frequency and severity of symptoms[51]. In case of symptoms suggestive of cardiac ischemia, patients should always be advised to seek medical care. This is why the miniECG algorithms should take into account any cardiac symptoms experienced by a patient.

The results of this study show the potential of the miniECG in the capture of ST-deviation during coronary artery occlusion. The fact that ST-deviation could be captured early and that miniECG showed overall ST-deviation of large magnitude in reference to 12-lead ECG, is very promising. Still, this needs to be confirmed for cardiac ischemia of different anatomical locations.

For the implementation of the miniECG in acute cardiac care, the miniECG should have high sensitivities for cardiac ischemia in different anatomical regions of the heart in humans. Capture ST-deviation in antero-septal infarction using the precordial electrodes of the miniECG is expected, as ST-deviation shows in ECG leads facing an ischemic zone. However, for the capture of ST-deviation in infarction of other anatomical cardiac regions, different positioning of the miniECG might be possible to optimally

capture ST-deviation. High specificities are important to prevent false positive referrals to acute clinical care as this will increase healthcare workload. Diagnostic criteria are needed to evaluate cardiac ischemia based on miniECG recordings, as lead configuration differs from current clinical standards. For the clinical 12-lead ECG, specific and sensitive criteria for the detection of cardiac ischemia exist that incorporate ST-elevation and or depression in specified leads, including thresholds based on age and gender[4]. The location of myocardial infarction can be deducted from the clinical 12-lead ECG as well. As the miniECG uses a new measuring method incorporating only four precordial electrodes, device specific criteria have yet to be developed. These criteria can be developed and evaluated through clinical research where the miniECG is compared between patients without and with cardiac ischemia with different locations and types of culprit lesions.

Conclusion

This study aims to investigate the capture of ischemic ST-segment changes by a new handheld 4-precordial electrode recording device (miniECG). We have observed that (i) the miniECG records high quality ECG showing ST-deviation during coronary artery occlusion. (ii) ST-deviation ≥1mm was observed earlier on the miniECG compared to 12-lead ECG and miniECG ST-deviation was of larger magnitude compared to the 12-lead ECG. (iii) ST-deviation shows two peaks around 10 and 30 minutes of occlusion after which ST-deviation decreases in a porcine occlusion model. These findings demonstrate the added value of the miniECG as a portable smartphone-sized ECG device in the early detection of cardiac ischemia. Diagnostic criteria and accuracy of the miniECG in relation to cardiac ischemia of different anatomical areas need to be evaluated further in clinical research.

4 Detection of myocardial ischemia using a novel set-up with four precordial electrodes: a pilot study

Introduction

Ischemic heart disease is a leading cause of death, accounting for almost 1.8 million annual deaths in Europe[4,8,50,52]. In acute myocardial infarction (AMI), cardiomyocyte necrosis leads to a rise in cardiac biomarkers, accompanied by supportive evidence such as clinical cardiac symptoms, ECG changes, or imaging suggestive of loss of viable myocardium. Clinical symptoms of AMI vary. These include chest pain and tightness, pain radiating to arms, shoulders, neck and jaw, nausea, sweating and dyspnoe[4,8,53].

AMI can be divided into two subtypes. ST-elevation myocardial infarction (STEMI) is a type of AMI where cardiac symptoms are accompanied by ST-segment elevation on the ECG. STEMI is defined in the Third Universal Definition of Myocardial Infarction as "ST-segment elevation in at least two contiguous leads with ST-segment elevation ≥ 2.5 mm in males < 40 years, ≥2 mm in men ≥ 40 years, or ≥ 1.5 mm in females in leads V2–V3 and/or ≥ 1 mm in the other leads"[53]. These criteria only apply in the absence of left bundle branch block (LBBB) and left ventricular hypertrophy (LVH)[53].

The second type of AMI is Non-ST-segment elevation myocardial infarction (NSTEMI). In case of NSTEMI, cardiac symptoms are present along with a rise in cardiac markers, however without persistent ST-elevation. Often, ECG changes other than persistent ST-elevation are present in NSTEMI. Examples of this are transient ST-segment elevation, persistent or transient ST-segment depression, T-wave inversion, flat T-waves, or pseudo-normalization of T-waves. However, in some NSTEMI patients the ECG is normal[8,53].

Treatment of AMI is directed towards rapid restoration of cardiac perfusion, with percutaneous coronary intervention (PCI) as the primary strategy[4,8,53]. AMI poses patients at high risk of developing ischemia induced life threatening arrhythmias such as ventricular fibrillation (VF)[4]. Emergency care of AMI therefore requires ECG monitoring and defibrillation in case of life-threatening arrhythmias.

Rapid treatment of AMI is essential to minimize ischemic damage to the myocardium and ultimately to minimize mortality and morbidity[5,6]. To improve time-to-treatment, pre-hospital ECGs play an important role. When AMI diagnosis is made in a pre-hospital setting, the catheterization laboratory can be activated in advance and fibrinolytic therapy can be started. Median time to treatment is significantly shorter for patients with a pre-hospital ECG and a suggestive trend for a lower risk of in-hospital mortality has been reported with pre-hospital ECG use[7].

Availability of 12-lead ECG with high sensitivity and specificity in the detection of AMI is limited to specific locations, such as the hospital, some general practitioners' offices and some nursing homes. Even where ECG devices are available, these might have to be retrieved from central locations, taking valuable time. A second challenge in the diagnosis of AMI is the time-dependent character of ST-segment changes suggestive of myocardial ischemia. A single ECG recording might miss the more dynamic ECG changes that might be detected with serial recordings[53,54].

A solution to both availability issues of current clinical ECG, could be the application of portable ECG devices, meaning easily accessible for a patient at any time and easy to operate without the need for a healthcare professional, However, portable ECG devices that are currently available have not yet been able to reach high sensitivities in the detection of AMI. Most currently available devices for cardiac home-monitoring are developed for the detection of rhythm disorders only and use 1-3 leads.[22] Because ST-segment changes are dependent on the location of the AMI and positioning of the ECG leads, multi-lead ECG is needed to reach high sensitivities[22]. The Apple Smart-watch ECG for example reaches low sensitivity of 34% in the detection of ST-segment and T-wave abnormalities[22].

The miniECG was developed to be used as a portable ECG device in the detection of the full spectrum of ECG abnormalities. It uses four precordial electrodes to record multi-lead ECG as discussed in ***Chapter 1***. The accuracy of the detection of myocardial ischemia using miniECG compared to 12-lead ECG has not yet been investigated. The implementation and clinical implications of the miniECG in hospital, pre-hospital and home-monitoring settings will largely depend on how accurately the miniECG signal can be used to detect myocardial ischemia. This pilot study was performed to investigate the capture of AMI of different anatomical locations by the miniECG.

Methods

This multicenter clinical study was declared non-WMO by the METC Utrecht (20-817/C). Patients were included in the University Medical Center Utrecht and Meander Medical Centre between the 26th of April 2021 and the 19th of February 2022. Inclusion and exclusion criteria are shown in **Table 4.1**. Written informed consent was retrieved after acquisition of recordings, as approved by the METC.

Table 4.1: Inclusion and exclusion criteria

Inclusion criteria	Exclusion criteria

• Age > 18 years
• Presenting to the Emergency Department with chest pain
• Evaluated to diagnose or rule out acute myocardial infarction
• Able to provide Informed Consent
	• Patients where the 12-lead ECG can is nondiagnostic for acute myocardial infarction:
	  ○ Continuous ventricular pacing
	  ○ Left ventricular assist device (LVAD)
	• Patients where no measurement can be performed (recent sternotomy (< 48 hours) or other anatomical restrictions)

Sample size

The sample size was calculated for estimating the area under the receiver operating curve (AUROC) for diagnostic studies with a single test. At a predicted prevalence of ST-elevation myocardial infarction of 30%, a margin of error of 0.07, alpha of 5%, power of 80% and expected AUROC of 0.9, the estimated required sample size was 342 patients[7].

Health data

Baseline values including age, gender, cardiovascular history and risk factors were retrieved from the electronic patient records. The final diagnosis (deducted from laboratory values, CAG and PCI documentation, cardiologists' conclusion and 12-lead ECG) was retrieved from the electronic patient records. To evaluate the ECG abnormalities with respect to the severity of the coronary artery occlusion, TIMI flow and stenosis grade were evaluated based on CAG. ECG metadata including time of ECG were included if available.

A 12-lead ECG (General Electric Mac 5500 (GE Healthcare, Chicago, IL, United States)) was recorded at arrival at the Emergency Department by nurses as part of routine clinical care. These ECGs were retrieved from the GE Healthcare MUSE software.

A miniECG recording (as described in ***Chapter 1***) was acquired by the same nurse just before or after acquisition of the 12-lead ECG. These miniECGs were acquired using the miniECG app, from where

recordings were sent to a secure SurfDrive (SURF, the Netherlands) environment. The miniECG was positioned in the mid-line, with the lower electrodes on the lower sternal border (**Fig. 1.2**).

Patients showing ST-segment abnormalities indicating STEMI or NSTEMI in the ambulance ECG, were referred directly to the catheterization lab for Coronary Angiography (CAG). The miniECG was acquired in the catheterization lab in this case. In these patients 12-lead ECG was not routinely recorded before the CAG. If available, a 12-lead ECG was used as a reference. In other cases the ambulance ECG served as a reference ECG and additionally the 1-lead monitoring ECG was evaluated for ST-deviation (ST-elevation and or reciprocal ST-depression).

MiniECGs were evaluated for rhythm, conduction and ischemia by two independent cardiologists. For the 12-lead ECGs, the clinical evaluation of the ECG by a cardiologist (in training) was used.

Filtering of miniECGs

Filtering was optimized from the prototype version after acquisition of the study data. The optimized filtering incorporated a polynomial curve fitting method to reduce baseline wander, with a high-pass, low-pass and a notch filter. Filtering parameters were optimized based on the study data to reduce baseline wander, 50Hz noise and high frequency noise, while retaining morphology of the ST-segment and QRS-amplitudes.

For the first step of the polynomial curve fitting method, the raw miniECG signals were filtered bidirectionally, using an 8^{th} order low-pass Butterworth filter with a cutoff frequency of 5Hz. 6^{th} degree polynomials were fitted to this low-frequency signal. This leaves signals that represents a large part of the baseline wander. These signals were deducted from the raw miniECG signals to reduce baseline wander.

Additionally, the resulting signals were filtered bidirectionally, using an 8^{th} order high-pass Butterworth filter with a cutoff frequency of 0.67Hz. A notch filter was applied at 50Hz with a quality factor of 5. To reduce high frequency noise, a low-pass Chebyshev filter of type II with an attenuation of 30dB and 6^{th} order at a cutoff frequency of 100Hz was applied bidirectionally.

Preliminary analysis

This analysis focused on the evaluation of miniECG quality and detection of ST-deviation in STEMI patients, NSTEMI patients and patients without cardiac ischemia. Differences in baseline characteristics between the three groups were investigated using Fisher's Exact Test, except for the baseline characteristics age and BMI, for which one-way ANOVA was performed.

Detection of ST-deviation was divided into three categories based on the two cardiologists' interpretation: ST-deviation observed by both cardiologists', disagreement on ST-deviation and no ST-deviation observed by both cardiologists. One-way ANOVA was used to investigate differences in BMI and time between the miniECG and reference ECG between these categories. Fisher's Exact Test was applied to investigate differences in gender, location of ischemia, TIMI-flow, culprit lesion and reference ECG ST-deviation between these categories.

Results

Between the 26th of April 2021 and the 10th of January 2022, miniECG recordings were acquired of 369 patients of whom 325 have signed informed consent. Out of these 325 patients, 70 STEMI cases, 37 NSTEMI cases and 218 patients without ischemia were identified based on electronic health records (**Table 4.2**).

Table 4.2: Baseline characteristics

Variable	STEMI (N=70)	NSTEMI (N=37)	No Ischemia (N=218)	*P*-value
Males (%)	83	70	63	0.007
Age (yr)	62	70	63	0.007
BMI	29	27	28	0.802
History of cardiovascular disease (%)	31	59	65	<0.001
Smoking (%)				
currently	26	14	17	0.234
in history	28	31	31	0.693
Hypercholesterolemia (%)	31	62	45	0.008
Hypertension (%)	30	54	52	0.004
Diabetes (%)	10	27	18	0.078

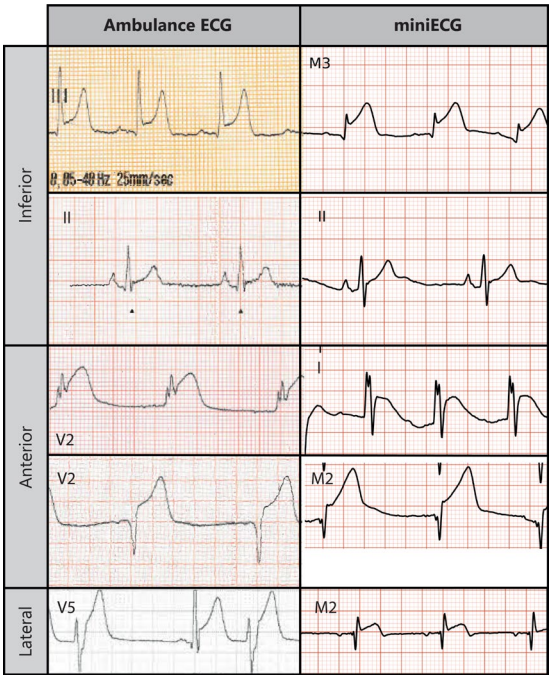

Figure 4.1: miniECG and 12-lead ECG ST-deviation with similar morphologies in cardiac ischemia of different anatomical locations.

MiniECG ST-deviation

81% of miniECGs were interpretable regarding ischemia according to the two cardiologists. 11% of the miniECGs were non-interpretable regarding ischemia due to disturbing noise or flat-lines. In 8% of ECGs, cardiologists disagreed on the interpretability of the miniECG regarding ischemia. No significant difference in miniECG quality was observed between the STEMI, NSTEMI and no ischemia subgroups (p=0.349). In **Table 4.3**, presence of ST-deviation in miniECGs of sufficient quality in the STEMI, NSTEMI and no ischemia subgroups are shown. ST-deviation was observed in 26 out of 54 high quality STEMI miniECGs (48%), in 2 out of 30 high quality NSTEMI miniECGs (7%) and in 3 out of 155 high quality no ischemia miniECGs (2%).

Examples of ST-elevation in different miniECG leads and corresponding 12-lead ECGS are shown in **Fig. 4.1.** While morphology of the QRS-complex and ST-segment are similar between 12-lead ECG and miniECG, differences in amplitudes can be observed. An example of this is the larger R-wave in lead III of the 12-lead ECG compared to lead M3 of the miniECG in anterior infarction in **Fig. 4.1.**

Table 4.3: Prevalence of miniECG ST-deviation and miniECG interpretability

	MiniECGs of sufficient quality for ischemia interpretation		
	STEMI (N=54)	**NSTEMI (N=30)**	**No ischemia (N=155)**
ST-deviation visible according to both cardiologists	48%	7%	2%
Disagreement on ST-deviation	19%	23%	15%
No ST-deviation visible according to both cardiologists	33%	70%	83%

MiniECG leads and ischemia location in STEMI patients

MiniECG ST-elevation was most prominent in leads I, II and V2 for anterior ischemia and ST-depression was most prominent in the M-leads (**Table 4.4**). On the contrary, the M-leads showed ST-elevation in inferior ischemia and especially in infero-posterolateral (IPL) ischemia. For lateral ischemia, ST-depression was observed in the M-leads. No miniECG ST-elevation was observed in lateral ischemia.

Table 4.4: Location of ischemia in relation to miniECG ST-deviation in STEMI patients

	ST-elevation visible (%)								ST-depression visible (%)							
	I	II	V1	V2	V3	M1	M2	M3	I	II	V1	V2	V3	M1	M2	M3
Anterior (N=15)	53	33	0	33	20	20	7	7	0	0	13	0	13	27	47	47
Anterolateral (N=7)	57	57	0	29	43	43	0	0	0	0	57	14	0	14	43	57
Lateral (N=2)	0	0	0	0	0	0	0	0	0	0	0	0	0	0	50	50
Inferior (N=14)	7	7	0	7	7	29	29	29	7	7	7	0	7	7	14	14
IPL (N=14)	0	43	0	0	43	64	57	57	29	0	0	36	0	0	7	7

Detection of ST-deviation in STEMI patients

An overview of miniECG ST-deviation in STEMI patients is shown in **Table 4.5**. Only TIMI-flow and ST-deviation at hospital arrival showed significant differences with respect to detection of ST-deviation using the miniECG ($p=0.023$ and $p<0.001$, respectively). The miniECG ST-deviation patients showed a lower TIMI flow compared to the patients where no miniECG ST-deviation was observed. ST-deviation at hospital arrival was often unknown, especially in the no ST-deviation and disagreement groups. Aborted STEMI, where ST-deviation disappears on the 12-lead ECG before CAG, occurred in 7 out of 21 cases (33%) showing no ST-deviation on the miniECG.

False negatives

In seven STEMI patients with TIMI flow 0, no miniECG ST-deviation was observed by two cardiologists (**Table 4.6**). In two of these patients ST-deviation had resolved on the reference 12-lead ECG before or at hospital arrival (**Fig 4.2, Fig 4.3**). In four of these patients the presence of ST-deviation at presentation was confirmed through 12-lead ECG or monitoring ECG during catheterization. For one patient, no 12-lead ECG was recorded at hospital arrival and the 1-lead monitoring ECG did not show ST-deviation. Therefore ST-deviation at hospital arrival could neither be confirmed or ruled out.

Table 4.5: Factors in miniECG ST-deviation in STEMI patients

ST-deviation on miniECG	Yes (N=26)	Disagreement (N=10)	No (N=18)	*P*-value
Mean BMI	28	25	30	0.114
Males (%)	88	90	83	0.871
Location of ischemia (N)				0.842
Anterior	7	3	5	
Antero-lateral	3	3	1	
Lateral	1	0	1	
Inferior	6	1	7	
Infero-lateral	2	2	0	
Infero-posterolateral	5	1	4	
Posterior	1	0	0	
Pan-ischemia	1	0	0	
Mean time between ECGs (min)	18	28	21	0.563
ST-deviation at hospital arrival (N)				<0.001
ST-deviation present at hospital arrival	25	5	5	
Aborted STEMI (still enzyme rise)	0	0	7	
Aborted STEMI (no enzyme rise)	0	0	0	
Unknown	1	5	6	
TIMI flow (N)				0.023
TIMI flow 0	20	6	7	
TIMI flow 1	3	0	0	
TIMI flow 2	1	2	3	
TIMI flow 3	1	2	6	
Not measured*	1	0	2	
Culprit lesion				0.708
LCA	1	0	0	
LAD	11	6	7	
RCA	6	3	7	
RCx	7	1	2	
No culprit identified*	1	0	2	

* No PCI performed. One STEMI patient diseased during the CAG before any culprit lesion was identified. Two NSTEMI patients showed insignificant stenosis during CAG and PCI was therefore not indicated.

Table 4.6: STEMI TIMI-flow 0 patients without miniECG ST-deviation

Time between miniECG and 12-lead ECG	ST-elevation at hospital arrival	Culprit	Location of ischemia	BMI	Cardiologist's evaluation notes
46	Resolution of ST-deviation	LAD	Anterior	38,74	
Unknown	Resolution of ST-deviation	LAD	Anterior	27,77	Biphasic T-wave
44	ST-deviation present	RCA	Inferior	Unknown	High voltage
Unknown	ST-deviation present	RCA	Inferior	27,17	
24	ST-deviation present	RCA	Infero-posterolateral	43,54	Low voltage
31	Unknown	RCx	Infero-posterolateral	31,35	
15	ST-deviation present	RCx	Infero-posterolateral	26,54	

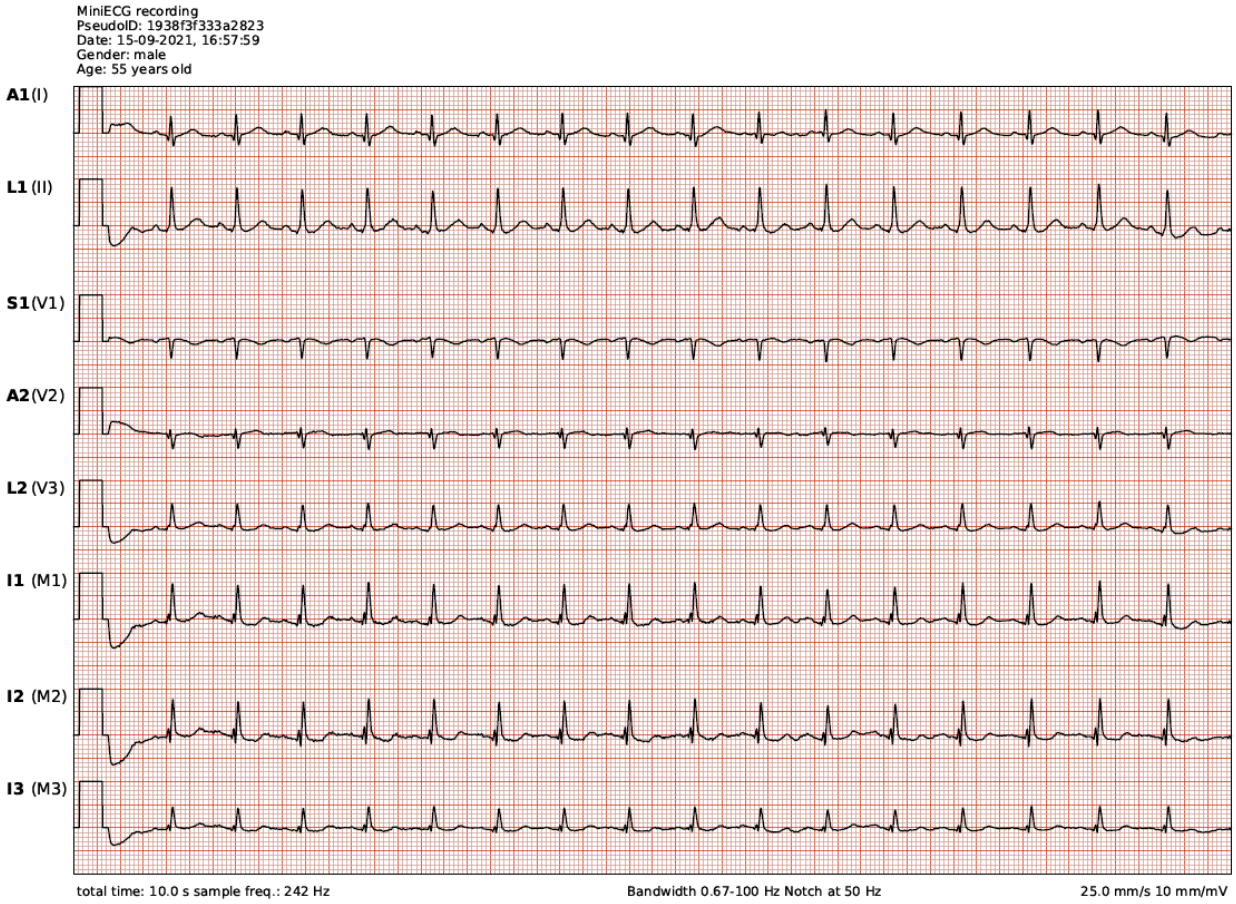

Figure 4.2: MiniECG of a patient with anterior STEMI with TIMI-flow 0 (first patient of Table 4.6) where the two cardiologists observed no miniECG ST-deviation.

a

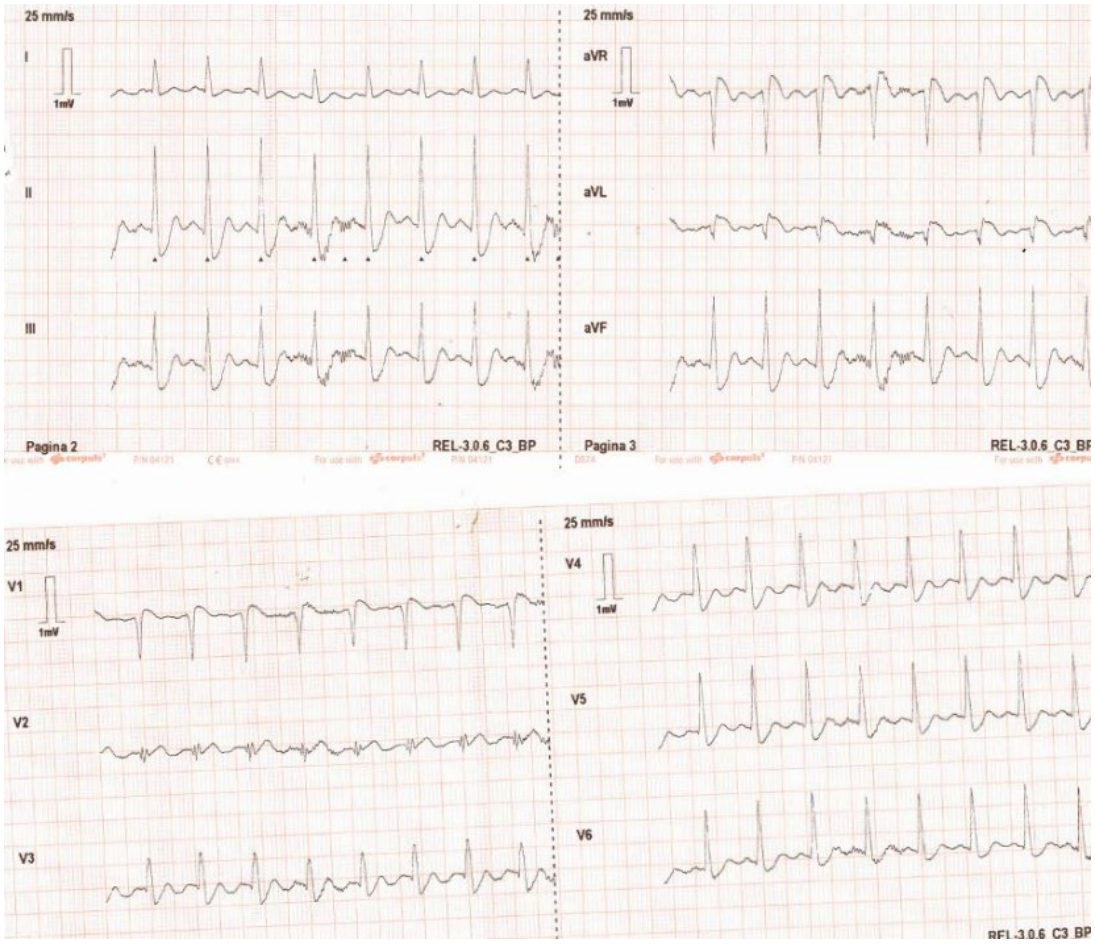

b

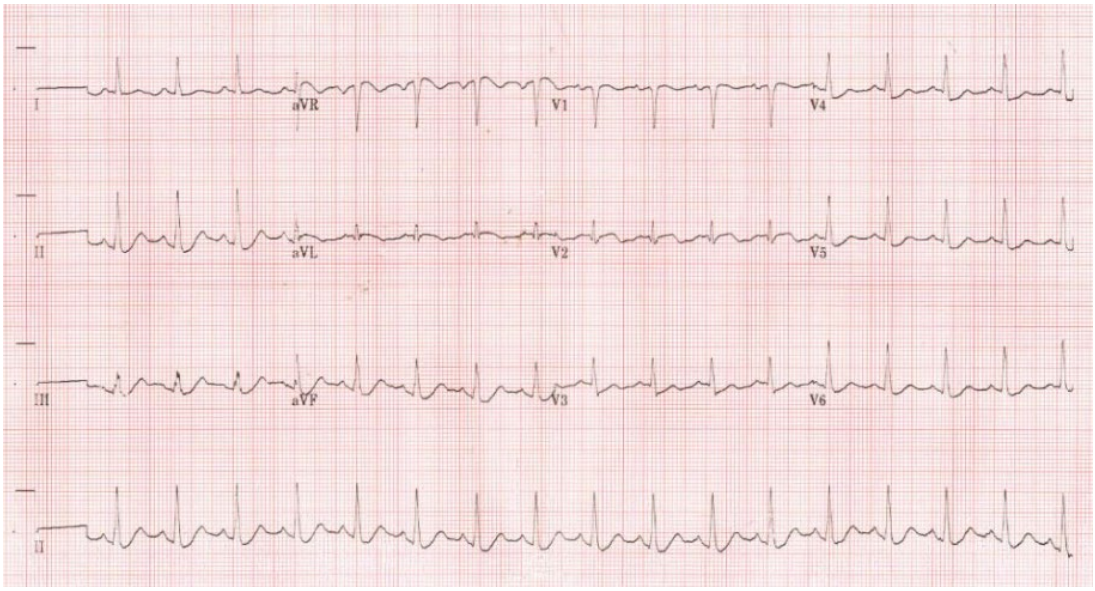

Figure 4.3: Resolution of ST-deviation in a patient with anterior STEMI with TIMI-flow 0 (first patient of Table 4.6). a. The first 12-lead ECG was recorded in the ambulance. b. The second 12-lead ECG was recorded in a peripheral hospital, from where the patient was referred to the UMC for PCI. The miniECG was recorded at arrival at the catheterization lab of the UMC Utrecht 46 minutes after the second 12-lead ECG. A large decrease in ST-deviation between the first and second 12-lead ECGs was observed.

Discussion

This study was performed to investigate the capture of ischemic ST-deviation by the miniECG in patients suffering myocardial infarction.

Preliminary analysis of the study data showed miniECG ST-deviation in 48% of ST-elevation myocardial infarction (STEMI) patients. Ischemia of different anatomical areas showed ST-elevation and or ST-depression in different miniECG leads, with IPL infarction showing ST-deviation in most leads, and lateral ischemia showing ST-deviation the least leads. Prevalence of miniECG ST-deviation in STEMI patients was related with TIMI flow. ST-deviation was more often confirmed at hospital arrival in patients with miniECG ST-deviation.

ST-deviation in STEMI patients

The capture rate of around 48% of STEMI patients is likely an underestimation of the true sensitivity of the miniECG in cardiac ischemia, which is supported by secondary findings of this study. An example of this is the significantly lower TIMI flows reported in miniECG ST-deviation patients, compared to patients where no ST-deviation was observed in the miniECG. When STEMI is diagnosed in the ambulance, fibrinolytic therapy is started immediately. If fibrinolytic therapy is started within one hour of symptoms onset, this results in abortion of 25% of STEMIs, meaning major resolution of ST-elevation and a lack of a subsequent enzyme rise more than twice the upper normal limit of creatine kinase[55,56]. When a thrombus is the primary cause of the occlusion, fibrinolytic therapy can result in a significant improvement of coronary artery flow, reflected both in the prevalence of ST-deviation at hospital arrival and in the TIMI flow determined in the catheterization lab.

The presence of ST-deviation may be confirmed through the monitoring ECG at the catheterization lab, but never ruled out, as this 1-lead ECG has low sensitivity for ischemia detection. Presence of ST-deviation was not confirmed more often in cases where ST-deviation was not captured by the miniECG, implying the possibility of absence of 12-lead ST-deviation in these patients.

Explaining confirmed false negatives

Subgroup analysis of patients with total occlusion (TIMI flow 0) may give rise to a more realistic estimate of sensitivity of the miniECG in the detection of ischemic ST-deviation. In these patients, resolution of ST-deviation before acquisition of the miniECG is rare, and therefore if ST-deviation is not captured, this is more likely due to the measuring method instead of resolution of ST-deviation. However, it should still

be noted, that as shown in the animal study in ***Chapter 3***, ST-deviation in complete occlusion decreases over time as well, especially after one hour of coronary artery occlusion. Two STEMI patients with TIMI flow 0 had resolution of ST-deviation confirmed through 12-lead ECG in this study as well. On the other hand, subgroup analysis of the STEMI TIMI-flow 0 subgroup poses risks of overestimation of sensitivity as well. As this subgroup exists of patient with more severe types of coronary artery occlusion, therefore ST-deviation of larger magnitude is to be expected, which might be easier to capture.

Of the seven patients not showing miniECG ST-deviation, four had confirmed ST-deviation at arrival, meaning these are false negatives. Inspection of these patients could therefore reveal factors in missing ST-deviation by the miniECG. Interestingly these are all patients with inferior or IPL infarction, which might indicate that the miniECG has a lower sensitivity in the detection of this type of infarction. One case showed low voltages in combination with high BMI. Amplification of the signals might still reveal ST-deviation in this patient. Otherwise the use of the miniECG should have an upper limit for BMI.

Non-ischemic ST-deviation

The number of miniECG ST-deviation cases in patients without ischemia (2%) is low. This indicates that the criterium 'ST-deviation indicative of ischemia' is likely much in line with existing 12-lead criteria as the >1mm criterium of this study was adopted from 12-lead criteria. Qualitative analysis of ST-deviation should be performed to optimize qualitative criteria for ischemic ST-deviation. However, it should still be noted that these criteria can never be 100% specific, the criteria always reflect a payoff between sensitivity and specificity. While ST-segment elevation on the ECG is a diagnostic hallmark for STEMI, this finding is not specific to STEMI. In young males, ST-deviation observed especially in the precordial leads, is most often not indicative of any cardiac abnormality. On the other hand many cardiac abnormalities, including ventricular aneurysm, myocarditis, pericarditis, Takotsubo cardiomyopathy can elicit ST-deviation[57]. The distinction between these diseases can be made using clinical reasoning and additional diagnostics[53,58].

Location of ischemic area

Ischemia of different anatomical areas showed similar capture rates by the miniECG in the preliminary analysis. This is interesting as a device using fewer leads might be prone to low capture rates for ischemia of certain anatomical areas. This might be explained by the difference between 12-lead precordial leads and miniECG precordial leads. In the 12-lead ECG, the WCT is located approximately at the center of the heart. With the relatively linear placement of the V1-V3 electrodes (in one line from the central chest to the

lateral chest wall), the differences in leads are in the horizontal plane. While miniECG leads V1-V3 are based on electrodes located at the approximate locations of the 12-lead V1-V3 electrodes, the Wilson's Central Terminal (WCT) is located at the center of these electrodes. This means miniECG-V1 is directed cranially towards the right atrium, V2 is directed cranially towards the left atrium and V3 is directed oppositely from V1, caudally towards the left ventricle. The directions of V1-V3 of the miniECG are therefore not really in the horizontal plan, but oblique towards frontal plane.

As explained in ***Chapter 3***, the observed magnitude of ST-deviation in specific leads can be explained by the solid angle theory; as a direct consequence of electrode position with respect to the ischemic currents. A lead directed perpendicularly with respect to the transitions of ischemic myocardium to healthy myocardium, shows most ST-elevation. For the 12-lead ECG, this means anterior ischemia is reflected in ST-elevation in the precordial leads. As the miniECG leads are directed more obliquely, this might explain a lower capture rate of anterior ischemia induced ST-deviation, compared to the 12-lead. On the other hand, this poses possibilities for the detection of inferior and lateral infarction, as confirmed by the similar miniECG capture rates of inferior and lateral ischemia shown in this preliminary analysis.

Competitor devices

There is an increasing interest in mobile ECG devices, aimed at self-use by patients. Currently, applications mostly lie in the detection of rhythm disorders such as atrial fibrillation (AF) [22]. This is not only beneficial for early detection of cardiac abnormalities; a recent publication has even shown the potential of mobile ECG devices in the reduction of urgent healthcare visits[59]. However, no mobile ECG devices with high detection rates in cardiac ischemia are yet available. A study on the Apple watch series 4 and 5 (Apple Inc, Cupertino, CA), primarily focusing on the detection of arrhythmias, showed limited ability of the ECG for the detection of ischemia with a sensitivity of 34% in the capture of ST-deviation as a secondary outcome[21]. This demonstrates that one-lead mobile ECG devices are not suitable in the detection of cardiac ischemia.

The only competitor device developed and validated for ischemia detection is the RELF method: a three-lead system using gel-electrodes, together with automated algorithms for ischemia detection for self-use by patients[60]. Sensitivities of 91%, 87% and 80% were reported for LAD, RCA and CX occlusion respectively at 60s of coronary artery occlusion onset. As the study design differs largely from this study, no comparison can be made between the miniECG ischemia detection rate and that of the RELF method.

The main reason for this is the varying time between occlusion onset and miniECG recording in the current study and the fact that miniECG was recorded in an overall later stage of occlusion. As the magnitude of ST-deviation varies largely and decreases over time, as discussed in ***Chapter 3,*** possibly even more with incomplete coronary artery occlusion. Use of fibrinolytic therapy, incomplete occlusion and coronary artery occlusion >75 minutes in this study might even result in less ST-deviation, lowering the chance of capture of ST-deviation at hospital arrival.

Limitations

Lack of simultaneous gold standard reference (12-lead ECG) is the largest pitfall of this study. As explained, ischemic ECG changes are highly variable and time dependent. This is why in cases without miniECG ST-deviation, it is not known whether this is false or true negative in this specific case.

ECG evaluation shows large inter-observer variability. Even experienced cardiologists show large degrees of disagreement, which is reflected by the large prevalence of disagreement regarding miniECG quality and ST-deviation in this study[2,11–14]. Therefore double-blinded assessment, with additional feedback by a third cardiologist in case of disagreement, is essential for a study like this. This is why no conclusions can be drawn until all miniECG with disagreement on quality or the presence of ST-deviation are evaluated by a third cardiologist.

Subgroup analysis within STEMI patients, for example TIMI flow subgroups or ischemia of various anatomical areas, is less precise and possibly less accurate because of the small number of patients.

Future perspective

AMI is an acute, life-threatening disorder, where patients benefit greatly from rapid intervention[4,8,50,52]. Mobile ECG techniques may be of great importance in improving time to treatment and to decrease the number of ischemia induced life arrhythmias, a large cause of acute cardiac death[4,61]. Based on this preliminary analysis, the added value of the miniECG in early diagnostics of cardiac ischemia cannot yet be assessed and after thorough analysis of the complete dataset, results might still be inconclusive for the reasons mentioned in the limitations section.

Nonetheless, this study shows the potential of the miniECG in detection of ischemia of all anatomical areas. Additionally, it identified possible relationships between missing miniECG ST-deviation in STEMI patients and TIMI flow, 12-lead ECG ST-deviation, BMI, and low voltages. Further research should minimize the time between the miniECG recording and the 12-lead ECG recording, for example through

recording of the miniECG directly in the ambulance at the same time of a 12-lead reference ECG. The influence of the measuring position of the miniECG should be evaluated, in males and females and in people with BMI>30 to investigate factors in low voltage ECGs.

Conclusion

The miniECG poses possibilities for early and repeated ECG acquisition early after the onset of cardiac symptoms. Preliminary analysis of the study data focused on the capture of ST-deviation by the miniECG in patients with and without cardiac ischemia. Capture rates of ischemia of different anatomical areas was similar in STEMI patients. However, miniECG ST-deviation was only observed in 48% STEMI patients. Missing miniECG ST-deviation was related with higher TIMI flow, absence of 12-lead ST-deviation at hospital arrival and possibly miniECG micro voltages as a result of high patient BMI.

More research into factors influencing miniECG ST-deviation is needed before the added value of the miniECG in the early detection of cardiac ischemia can be established. Time between miniECG and 12-lead reference ECGs should be minimized to mitigate the dynamic nature of ST-segment changes during cardiac ischemia as a factor in the capture of ST-deviation.

5 Detection of ECG abnormalities using a novel set-up with four precordial electrodes

Introduction

In ***Chapter 4***, the feasibility of the 4-electode precordial ECG measurement to detect myocardial ischemia is discussed. The preliminary analysis of the pilot study shows that the novel device with four precordial electrodes captures ischemic ST-elevation in patients with inferior, lateral and anterior myocardial infarction. The next step in the clinical validation of the miniECG is to demonstrate the feasibility of a 4-electrode precordial ECG measurement to detect the full spectrum of cardiac abnormalities.

For the 12-lead ECG, elaborate guidelines exist for the interpretation of the ECG[62–67]. In general, ECG abnormalities can be divided into three categories: rhythm disorders, conduction disorders and ischemia. Whereas one lead is sufficient for the evaluation of many conduction disorders, various rhythm disorders exist where multiple leads of the 12-lead ECG are needed to draw conclusions of the mechanism and origin of the rhythm disorder. As the miniECG uses only four precordial electrodes in a different set-up to measure multi-lead ECG as discussed in ***Chapter 1***, new criteria are needed to use the miniECG for diagnosing cardiac abnormalities.

The aim of this study is to demonstrate the feasibility of using the 4-electrode precordial ECG measurement in comparison to clinical standard 12-lead ECG in its ability to detect ECG abnormalities. This preliminary analysis focusses on qualitative assessment of 12-lead ECGs and miniECGs showing various abnormalities, to gain insight in the differences and similarities of both ECG devices.

Methods

This clinical study was declared non-WMO by the METC Utrecht (21-763/C). Patients were included in the University Medical Center Utrecht from the 15th of November 2021 onwards. Inclusion and exclusion criteria are shown in **Table 5.1**.

Table 5.1: Inclusion and exclusion criteria

Inclusion criteria	Exclusion criteria
• Age > 18 years • Undergoing 12-lead ECG • Able to provide Informed Consent	• Patients where no measurement can be performed (recent sternotomy (< 48 hours) or other anatomical restrictions)

Sample size calculation

The primary endpoint of this clinical study is detection of all cardiac ECG abnormalities by the miniECG compared to the reference standard 12-lead ECG. ECG abnormalities have highly varying incidences (**Supplement S5.1**). A sample size was calculated based on the prevalence of second-degree AV block as the smallest class. For the ECG abnormalities with lower incidence, it is expected that separate studies targeting these abnormalities are needed to reach sufficient inclusions.

Second degree AV-block has an expected incidence of 0.53% in the research population. When aiming at a power of 80%, alpha of 0.05, expected sensitivity of 0.95 and marginal error of 0.05, 74 patients with a second-degree AV block are needed. This translates to a total of 13962 patients.

Electrocardiography

A 12-lead ECG (General Electric Mac 5500 (GE Healthcare, Chicago, IL, United States)) is recorded at arrival at the Emergency Department by nurses as part of routine clinical care. These ECGs are sampled at 500Hz and filtered to a bandwidth of 0.05 to 150 Hz. The ECGs are retrieved from the GE Healthcare MUSE software used in the UMC Utrecht.

A miniECG recording (as described in ***Chapter 1***) is acquired by the same healthcare professional before or after acquisition of the 12-lead ECG. During recording, the lower two electrodes of the miniECG were positioned in the mid-line at the lower sternal border (**Fig. 1.2**). These miniECGs are acquired using the miniECG app, digitally filtered (as described in ***Chapter 4)*** and sent to a secure SurfDrive (SURF, the Netherlands) environment.

Organization of study

The study was rolled out starting at the heart-function department of the UMC Utrecht. A section of this department is dedicated to the routine acquisition of ECGs. If logistics allow, based on availability of miniECG devices and technical support by the miniECG team, the study will be extended to the cardiology

outpatient clinic, cardiology ward, and other 12-lead ECG machines that are available throughout the non-cardiology departments of the UMC Utrecht.

Preliminary analysis

The first goal of this preliminary analysis was to define criteria for normal sinus rhythm (SR) for the miniECG. For this all available miniECG recordings of patients with 12-lead ECG labeled normal SR by the GE algorithm were identified. MiniECGs with sufficient quality, meaning distinguishable P-wave and T-waves in at least 5 leads, were selected for further analysis. For these ECGs, P-wave polarity, and T-wave polarity were evaluated. Regarding T-waves, positive polarity was defined as maximum T-wave amplitude >1mm and minimum T-wave amplitude >-1mm with respect to baseline. Negative polarity was defined as maximum T-wave amplitude <1mm and minimum T-wave amplitude <-1mm with respect to baseline. Biphasic polarity was defined as >1mm positive and minimum T-wave amplitude <-1mm with respect to baseline. Isoelectric polarity was defined as maximum T-wave amplitude <1mm and minimum T-wave amplitude >-1mm with respect to baseline. For P-wave polarity, the same conventions were applied, however, with a threshold of 0.5mm. R-wave amplitude and RS-amplitude were calculated for the perpendicular miniECG leads I and M1 and compared to the QRS-axis as calculated by the GE algorithm.

Secondly, patients with 12-lead ECG labeled with common abnormalities by the GE algorithm were selected as case studies. For these patients, one miniECG beat was selected and visually compared with one beat of the 12-lead ECG and 12-lead criteria for the anomalies were translated to the miniECG recordings.

Results

47 patients with normal SR ECG on GE labels were identified. In 9 of these patients, miniECG quality was insufficient, meaning no P-wave and T-waves could be distinguished in at least 5 leads. For the 38 patients with miniECG recordings of sufficient quality, P-wave and T-wave polarity is depicted (**Table 5.2**).

P-waves could be distinguished (positive, negative or biphasic P-waves) in 80% of leads. In 12% of leads P-waves were flat and in 8% of leads, P-waves could not be distinguished due to the presence of high frequency noise or baseline wander. T-waves and could be distinguished (positive, negative or biphasic T-waves) in 77% of leads. In 9% of leads P-waves were flat and in 14% of leads, T-waves could not be distinguished due to the presence of high frequency noise or baseline wander.

Normal sinus rhythm case study

A case study of normal sinus rhythm (**Fig. 5.1**) shows large differences between miniECG leads and 12-lead ECG leads. In the miniECG QRS-amplitudes are smaller compared to the 12-lead ECG, especially for leads I (3.5mm vs. 9mm), V1 (5mm vs. 14.5mm) and V2 (4.5mm vs. 12.5mm). The 12-lead ECGs show large differences between R-wave and S-wave amplitudes within leads. In the 12-lead ECG, normal R-wave progression was observed with a transition of the S-wave having a larger amplitude to the R-wave having a larger amplitude between leads V3 and V4. For the miniECG, no V4-V6 leads are available and this phenomenon could therefore not be evaluated. MiniECG leads mostly show equal R-wave and S-wave amplitudes within leads.

P-waves can be distinguished in all leads of this case study, except in V2 for both the miniECG and 12-lead ECG. T-waves can be distinguished in all leads except M2 and M3 for the miniECG, most often due to baseline wander. For the 12-lead ECG T-waves are visible in all leads. Polarity of P-waves, the QRS-complex and T-waves differs largely between the miniECG leads and corresponding 12-lead ECG leads. The miniECG V2-lead for example shows a QS pattern, while the 12-lead ECG shows a normal RS pattern, with a larger S-wave amplitude compared to the R-wave amplitude. Another example is the T-wave, which is of opposite polarity in V2 of the miniECG and the 12-lead ECG. PQ-interval, QRS-duration and QT-interval are visually similar between miniECG and 12-lead ECG, with 0.16s, 0.1s and 0.340s respectively.

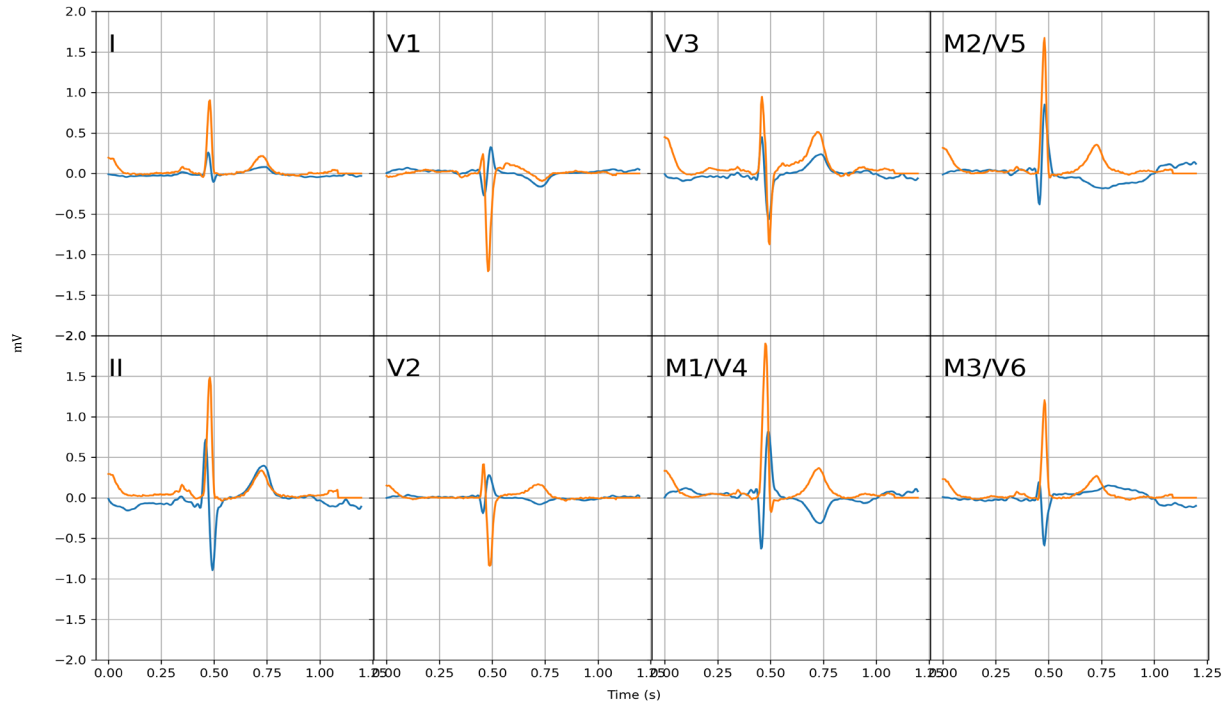

Figure 5.1: Example of a normal sinus rhythm ECG. A comparison between the miniECG (blue) and 12-lead ECG (orange).

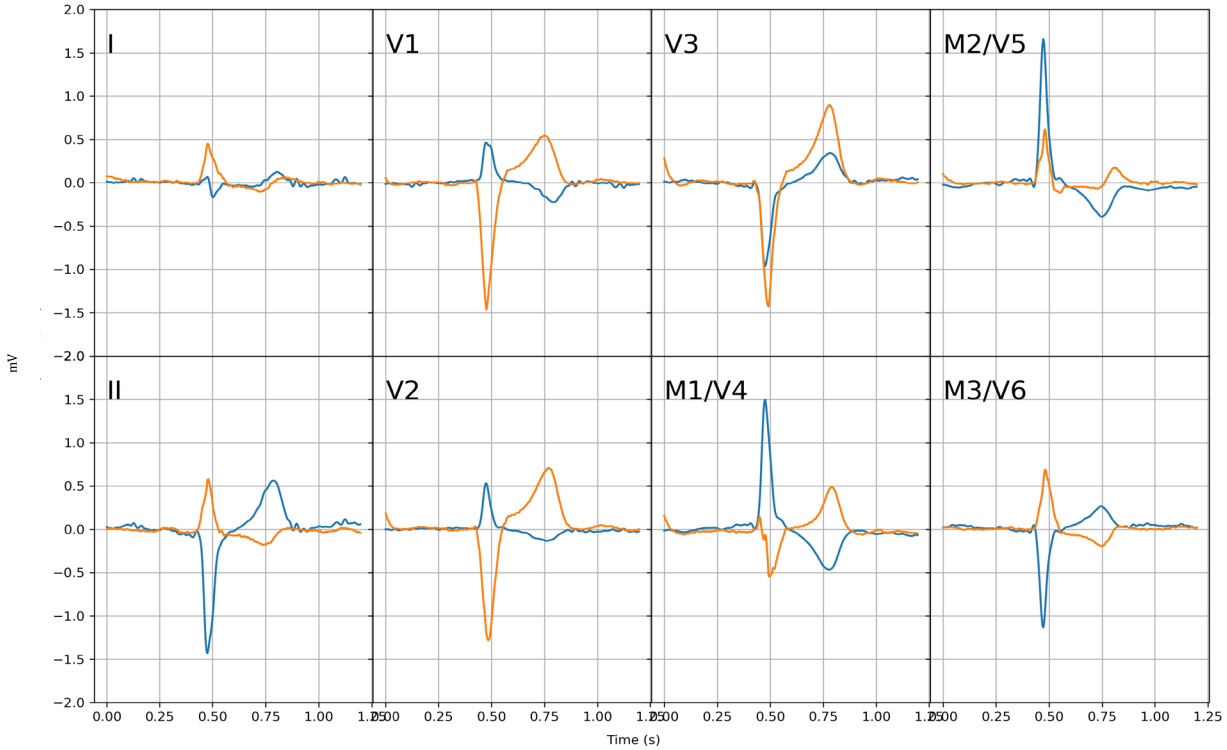

Figure 5.2: Left bundle branch block (LBBB) ECG. A comparison between the miniECG (blue) and 12-lead ECG (orange).

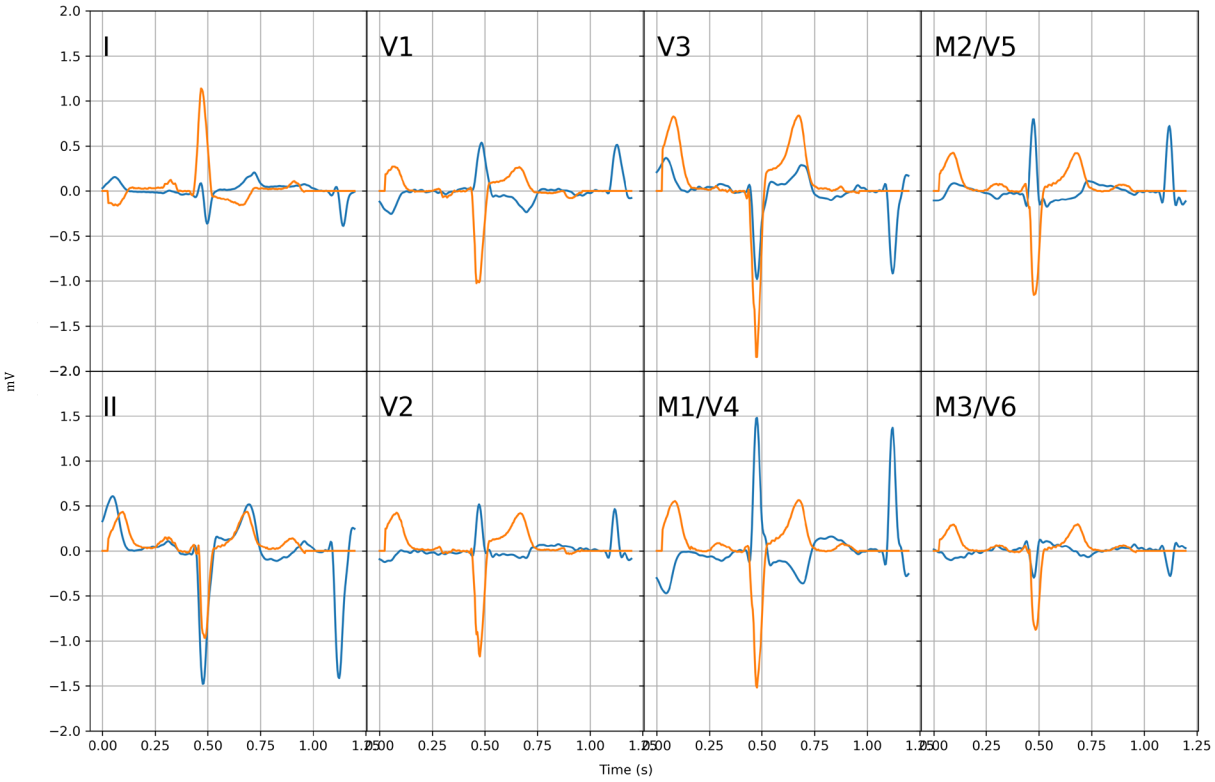

Figure 5.3: Left anterior fascicular block ECG. A comparison between the miniECG (blue) and 12-lead ECG (orange).

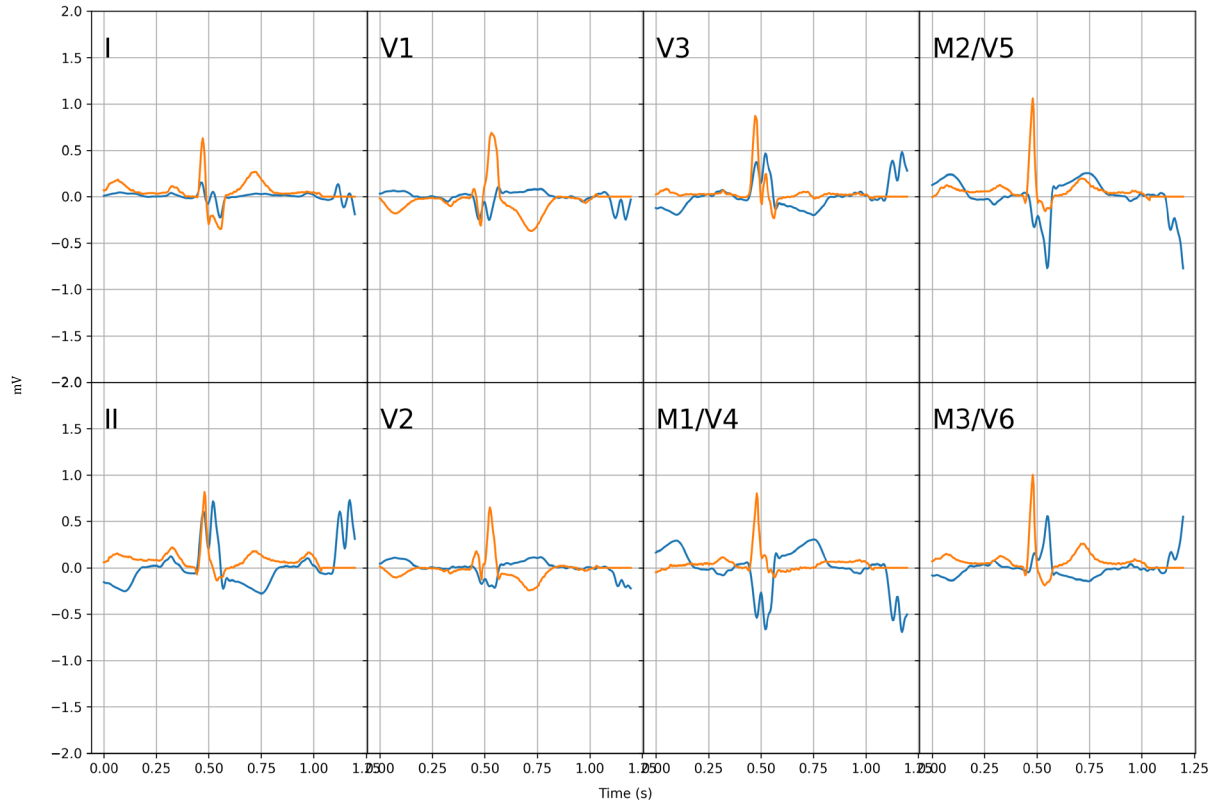

Figure 5.4: Right bundle branch block (RBBB) ECG. A comparison between the miniECG (blue) and 12-lead ECG (orange).

P-wave and T-wave polarity in normal SR

For the patients with normal sinus rhythm, P-waves were predominantly positive in miniECG leads I, II, V3, M1, M2 and M3. P-waves were predominantly negative in lead V1 and either negative or flat in V2. MiniECG T-waves were predominantly positive in leads I, II, V3 and M1. For leads M2 and M3, T-wave morphology varied largely. Leads V1 and V2 showed negative T-waves in the vast majority of patients (**Table 5.2**).

Table 5.2: P-wave and T-wave morphologies in patients with SR

	P-wave								T-wave							
	I	**II**	**V1**	**V2**	**V3**	**M1**	**M2**	**M3**	**I**	**II**	**V1**	**V2**	**V3**	**M1**	**M2**	**M3**
Positive	23	37	1	0	32	36	32	32	26	35	0	2	35	35	15	7
Negative	0	0	36	11	1	0	1	0	0	0	36	20	0	1	8	10
Biphasic	0	0	0	0	0	0	0	0	0	0	0	0	0	0	4	3
Isoelectric	6	0	1	24	2	0	1	3	0	0	0	11	2	1	5	7
Not determined	9	1	0	3	3	2	4	3	12	3	2	5	1	1	6	11

Case studies left bundle branch block

The case study of a patient with Left bundle branch block (LBBB) shows prolonged QRS-duration of 0.145s in both the 12-lead ECG and miniECG (**Fig. 5.2**). Broad monomorphic R-waves were observed in leads I and V6 with no Q-waves in the 12-lead ECG. Broad monomorphic S-waves were observed in V1 of the 12-lead ECG. This is in line with criteria for LBBB on the 12-lead ECG. On the contrary, miniECG lead I showed small R-waves with large S-waves. MiniECG lead V1 showed large R-waves in the miniECG. Deep S-waves were observed in the other leads of the miniECG, specifically in leads II, V3 and M3. T-wave polarity of these leads was, however, different from leads showing deep S-waves in the 12-lead ECG, showing dissimilarity of the two. 12-lead ECG showed approximately 2mm ST-deviation in leads V1-V3. This ST-elevation was not observed in any of the miniECG leads.

A case study of a patient with Left anterior fascicular block (LAFB) showed qR-complexes in lead I and small R-waves and deep S-waves in lead II (**Fig 5.3**). In the miniECG the LAFB case study shows similar QRS morphology as the LBBB case study, however with a shorter QRS-duration of 110s.

Case study right bundle branch block

The case study of a patient with right bundle branch block (RBBB) shows prolonged QRS-duration of 0.145s in 12-lead ECG and miniECG (**Fig. 5.4**). An RSR' pattern was observed in the 12-lead ECG V1-3 leads. A wide,

slurred S-wave was observed in lead I of the 12-lead ECG. For the miniECG leads II, V3, M1, M2, and M3 showed an RSR' pattern. Leads V1 and V2 showed slurred S-waves.

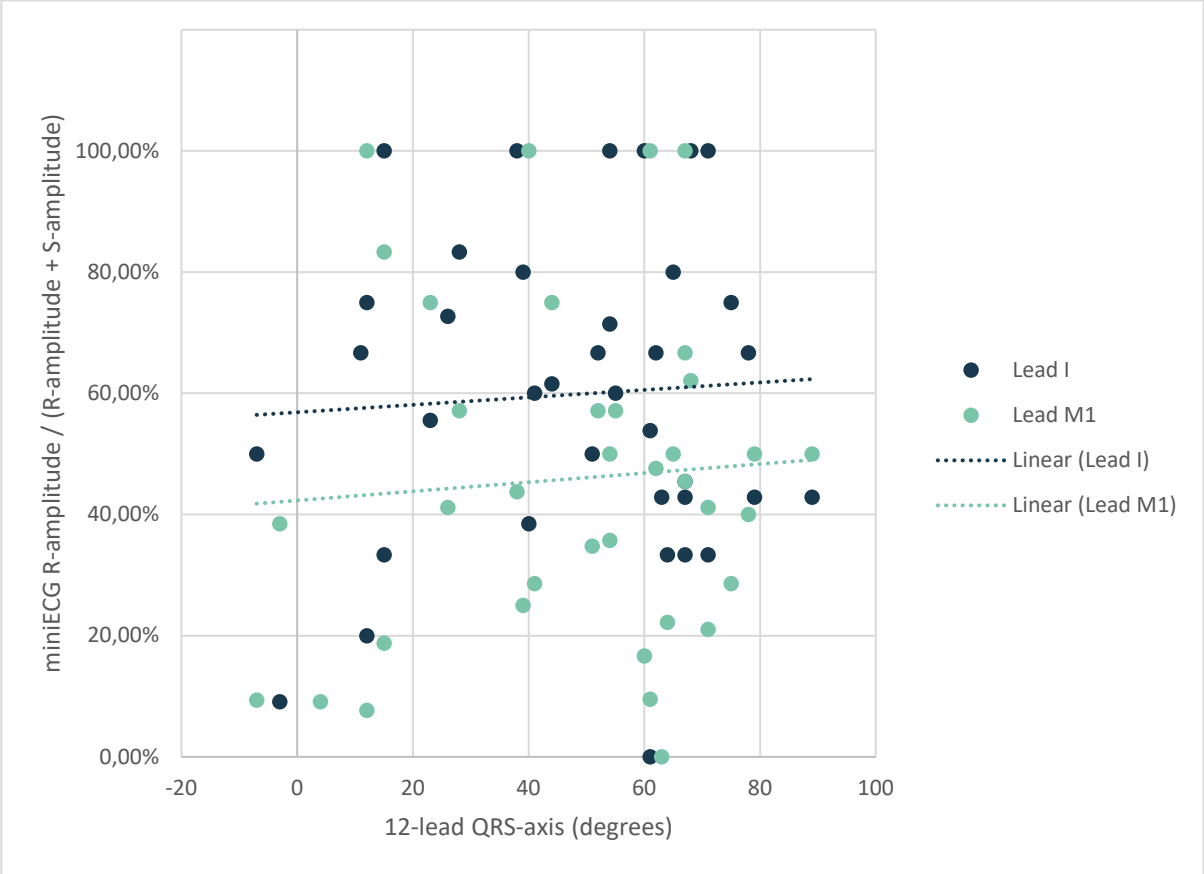

Figure 5.5: R-wave amplitude as a percentage of the RS-amplitude, visualized for both lateral lead I and inferior lead M1 of the miniECG. The relationship of these parameters with the QRS-axis as defined by the GE algorithm [71] is shown.

QRS-axis

The R-wave amplitude as a percentage of the RS-amplitude varied largely (0-100%). No relation between the R-wave amplitude as a percentage of the RS-amplitude in leads I and M1 of the miniECG and the 12-lead QRS-axis was observed (R^2=0.0034 and R^2=0.0046, respectively).

Discussion

This preliminary analysis focused on investigating criteria for normal SR on the miniECG and the evaluation of ECG abnormalities. P-waves are positive in miniECG leads II, V3, M1, M2, positive or flat in I, negative in V1 and negative or flat in V2. T-waves are positive in leads I, II, V3 and M1, negative in V1 and V2, and have varying polarities in M2 and M3.

Secondly, MiniECG showed typical RSR morphologies and wide slurred S-waves in RBBB and broad monomorphic S-waves and R-waves in LBBB. However, these morphologies were not observed in the leads on which 12-lead criteria for these abnormalities are based. Thirdly, conduction times (PQ-interval, QRS-duration and QT-interval) were similar for the four case studies presented based on visual assessment.

Normal SR criteria

As P-wave polarity and T-wave polarity vary very little in normal SR in the miniECG, these findings can be used to define preliminary criteria for normal SR. For the 12-lead ECG, criteria for normal SR not only include P-and T-wave polarity. The definition of normal SR in the 12-lead ECG includes criteria on amplitudes of waves, morphology of waves, conduction times, frequency and regularity as well.

Some 12-lead ECG normal SR criteria are very likely directly to the miniECG. For example, one normal SR criterium is a QRS frequency of between 60-100bmp, and that every QRS-complex has to be preceded by a P-wave. As P- QRS- and T-waves can be easily identified in the miniECG recordings, the QRS frequency can be determined and the occurrence of P-waves can be stated. The same accounts for the morphology of the P-waves. For the P-wave to originate from the same area (sinus node), all P-waves should have similar morphology.

The case studies showed similar conduction times between miniECG and 12-lead ECG, suggesting that criteria for conduction intervals for the 12-lead ECG can be directly translated to the miniECG. It is known that conduction times depend slightly on the positioning of the electrodes. For example QT-interval is usually measured in lead II of the 12-lead ECG, but when measured in precordial leads, this can lead to differences of 0.02-0.03s[68,69]. These small differences are not important when the ECG is assessed visually, which was confirmed by the visual assessment of the cases studies, meaning the standard 12-lead ECG criteria can likely be translated directly to the miniECG for visual assessment (a PQ-interval of 0.120-0.200s, a QRS-duration of 0.060-0.100s). QT-intervals are usually corrected for the QRS-frequency resulting in a QTc with normal values between 0.390-0.450s[70].

Dissimilarities of miniECG and 12-lead ECG leads

While MiniECG showed typical RSR morphologies and wide slurred S-waves in RBBB and broad monomorphic S-waves and R-waves in LBBB, these were observed in other leads than specified in 12-lead criteria. This suggests large dissimilarities between miniECG and 12-lead ECG leads. Based on anatomical positions lead names were defined in the development in the miniECG. Leads V1-V3 are measured using electrode positions comparable to the 12-lead ECG leads V1-3 and were therefore named accordingly. Leads I and II of the miniECG were developed to reflect the directions of the 12-lead ECG leads I and II. However, these examples show large differences between the miniECG and corresponding 12-lead ECG leads. On top of this, when ECG leads of the miniECG and 12-lead ECG are matched based on QRS-morphology, T-wave and P-wave still show differences in morphology and even polarity. This means that lead names cannot just be rearranged to increase similarity between the miniECG and 12-lead ECG, but more complex transformation of the miniECG is needed.

When looking at the lead configuration of the miniECG these findings can be explained. While leads V1-V3 are based on electrodes located at the approximate locations of the 12-lead V1-V3 electrodes, the Wilson's Central Terminal (WCT) is located approximately at the center of these electrodes. This means V1 is directed cranially towards the right atrium, V2 is directed cranially towards the left atrium and V3 is directed oppositely from V1, caudally towards the left ventricle. In the 12-lead ECG, the WCT is located approximately at the center of the heart. With the relatively linear placement of the V1-V3 electrodes (in one line from the central chest to the lateral chest wall), the differences in leads are in the horizontal plane. This results in the typical R-wave progression, where generally the R-wave amplitude increases from V1-V6 and the S-wave amplitude decreases, with a transitional point between V3 and V4. As the directions of V1-V3 of the miniECG largely vary not only in the horizontal plane, but in the frontal plane as well, these leads capture the activity of the heart in a majorly different way.

As all leads of the miniECG are recorded precordially and with electrodes positioned closely to each other within the anatomical borders of the heart, it is to be expected that part of the activity of the heart is always away from the electrode and part is in the direction of the lead. This may explain that the case study of normal SR shows R- and S-waves of similar magnitude within all leads of the miniECG.

Non ischemic ST-deviation occurs often in case of LBBB, and was observed in the LBBB case study in te 12-lead ECG. However, the miniECG only showed this in a much lesser extent. It is not clear from this study whether and how this is indicative of capture of ischemic ST-deviation by the miniECG.

QRS-axis and positioning of the miniECG

The investigation of the relation between R-wave and S-wave amplitudes in the miniECG leads I and M1 and the 12-lead QRS-axis as the output of the GE CIE, did not show a clear relation. For the lateral lead I, a QRS-axis of approximately 0 degrees should correlate with R-waves of the largest amplitude. The amplitude of the R-waves should be lower by a factor cosine of the angle for larger or smaller heart axes. As lead M1 is directed caudally, a larger QRS-axis should result in larger R-wave amplitudes in this lead. Nonetheless, both phenomena were not observed, indicating large variations of positioning of the miniECG between patients, or a non-optimal measuring method regarding the positioning of the miniECG in respect to the heart in general as discussed above.

Interestingly, P-wave polarity and T-wave polarity showed very little variation in normal SR. Normal SR includes the criterium of a normal QRS-axis, meaning a QRS-axis between -30 degrees and 90 degrees. As P-and T-wave polarity often show concordance with the QRS-complex, variability in QRS-axis is expected to translate into variability in P- and T-wave polarity.

Limitations

The case studies selected for this preliminary analysis only show anecdotal evidence regarding the ECG abnormalities discussed. Variation within one type of ECG abnormality is therefore not yet known. This is why, no criteria for the abnormalities can be deducted from these examples yet and more data is needed to be able to draw conclusions. Additional criteria for normal SR are needed as well, such as criteria on P-wave, QRS- and T-wave amplitudes.

The QRS-axis is a composite parameter in which R-wave and S-wave amplitudes of different leads play a role. GE does not elaborate on the mathematical methods behind the QRS-axis calculation. Direct comparison of QRS-amplitudes of the miniECG and 12-lead ECG could provide more insight into the (dis)similarities. The possibility of QRS-axis calculation based on the miniECG should be researched further.

While the criteria for normal SR in this research presented are expected to have high sensitivity based on this preliminary analysis, the specificity of criteria still has to be investigated using ECG examples showing abnormalities. Additionally, the clinical relevance of abnormalities regarding these criteria should be researched. For example, an isolated T-wave inversion in lead V1 is common. It is generally concordant with the QRS-complex in this lead. Isolated T-wave inversions also occur in leads V2, III, aVL or aVF. T-wave inversion visible in two anatomically contiguous leads most often indicates pathology. Various mechanisms

underlie T-wave inversion, such as myocardial ischemia, ventricular strain, hypertrophic cardiomyopathy and various conduction disorders[71]. Each mechanism has its clinical significance and would be clinically relevant to be able to diagnose based on criteria for the miniECG.

Future perspective

If the number of planned inclusion is reached, the accuracy of the miniECG in the detection of the specified ECG abnormalities (**Supplement S5.1**) can be determined and criteria for normal SR can be optimized. Secondly, the translation of the miniECG leads into leads resembling the 12-lead ECG can be investigated further, making the translation of 12-lead criteria into miniECG criteria easier.

Implementation of the miniECG in pre-hospital setting is largely dependent on the availability of automated algorithms for interpretation of the miniECG. While miniECG recordings by patients, could be easily sent to healthcare professionals in the future, this would ultimately increase workload and healthcare costs. To truly improve availability and accessibility of the ECG in pre-hospital settings, algorithms for diagnosis and triage should be incorporated.

Construction of median beats based on the 10s miniECG recordings may be of great help in the analysis of study data and in the development of algorithms for automated ECG analysis. Median beats are calculated by averaging the primary beats of an ECG recording, thereby minimizing noise in the ECG[17]. ECG conduction time- and morphology measurements based on a median beat generally show superior accuracy compared to ECG measurements based on each beat individually[72]. However, as median beat algorithms are not disclosed by ECG companies, such algorithms are not readily available. A median beat algorithm was developed in the UMC Utrecht, however, this needs to be validated before it can be used to construct median beats.

As results suggest inaccuracy of the miniECG in the calculation of the QRS-axis in different patients, it is interesting to investigate whether the QRS-axis within one patient shows less variance. If the QRS-axis varies largely between patients, but not within one patient, this would suggest that the miniECG can be recorded consequently at one anatomical position. The interpatient variance in the location of the heart compared to the torso would then be the cause of large interpatient variance. As the miniECG only records precordially, these differences are magnified compared to when the limb leads of the 12-lead ECG are used.

To get more insight into whether the miniECG can be recorded at one anatomical position consequently, sequential miniECGs can be recorded and compared in one patient. This would not only be

crucial in detection of changes in the QRS-axis, but also for the application of different criteria for hypertrophy, in which QRS-wave amplitudes play a large role. In the detection of ECG abnormalities, especially for the miniECG, the recording of sequential EGCs could be of great importance. If the QRS-axis is highly variable within one patient, this suggests that the measuring position of the miniECG is not reproduceable. This would imply the need for additional guidance in the acquisition of the miniECG.

Lastly, differences between the miniECG and 12-lead ECG could create new possibilities which should be researched. For example, measuring at a different position might lead to higher sensitivities for certain cardiac abnormalities. As the miniECG is positioned more towards the atria, atrial activation could be better visible on the miniECG. This cannot be confirmed through comparison with 12-lead ECG and comparison to health outcomes or more invasive techniques such as cardiac electrophysiology could be researched.

Conclusion

MiniECG recordings of patients with normal SR show small variation in P-wave morphology and T-wave morphology and therefore a draft definition of normal SR can be developed for the miniECG. For normal SR, every QRS-complex is preceded by a P-wave, that is positive in miniECG leads II, V3, M1, M2, positive or flat in I, negative in V1 and negative or flat in V2. T-waves are positive in leads I, II, V3 and M1, negative in V1 and V2, and can have any polarity in M2 and M3. Sensitivity and specificity of these criteria for the detection of SR have yet to be validated in a separate research population, as well as the clinical implications of negative T-waves. The case studies presented in this study show the versatility of the miniECG in detection of various ECG abnormalities. More research is needed to investigate criteria and accuracy of the miniECG in detection of abnormalities.

6 General conclusions and recommendations

The studies presented in this thesis were set-up to focus on the diagnostic capabilities of the miniECG. The miniECG was designed to bring 12-lead ECG diagnostic accuracy to the patient home, in the form of a portable, easy-to-use device. In contrast to currently available ECG devices for patient-use, the miniECG was designed not only for the detection for rhythm disorders, but for the challenge of ischemia detection as well. This is why the first steps of the validation of the miniECG focused on firstly on the detection of cardiac ischemia.

Validation of the miniECG

A pre-clinical study, as described in ***Chapter 3***, showed the capabilities of the miniECG in recording high quality ECG, showing ST-deviation during coronary artery occlusion. Ischemic ST-segment changes were investigated during onset, presence and following coronary artery occlusion through comparison with the standard 12-lead ECG in a porcine model of myocardial infarction. ST-deviation was observed earlier and deviation was of larger magnitude compared to 12-lead ECG. This shows proof-of-concept of the miniECG in ischemia detection. Next to this, the experiments gave insight into the dynamic nature of ST-deviation in coronary artery occlusion. Peaks in ST-deviation were observed, and ST-deviation decreased after 40 minutes of occlusion. The time-dependent character of ST-segment changes in cardiac ischemia emphasizes the added value of portable and smartphone sized ECG devices. As this study suggests, ST-deviation might be largest and therefore easiest to capture on the ECG in the first 40 minutes of cardiac ischemia. In case of incomplete coronary artery occlusion, ST-deviation might vary even more. The miniECG poses opportunities for easy follow up through repetition of ECG in patients with initial non-diagnostic ECG.

Results of the animal study cannot be directly translated from the porcine model to humans. The positioning of the porcine heart in relation to the chest is different compared to humans, as well as the anatomy of the conduction system and electrophysiological properties[43,44]. This is also why sensitivity of the miniECG in the detection of ischemia in humans cannot be estimated based on this study. To explore the capabilities of the miniECG regarding ischemia detection in ischemia of different anatomical areas, a clinical pilot-study was performed, as discussed in ***Chapter 4***. Preliminary analysis of the available study data showed similar miniECG capture rates of ischemia of different anatomical areas in STEMI patients. MiniECG ST-deviation was only observed in 48% STEMI patients. Higher TIMI flow, not documented ST-

deviation on 12-lead ECG, BMI and miniECG low-voltages are possible factors in missing miniECG ST-deviation and should be further investigated. A more reliable estimate of the sensitivity of the miniECG can be obtained as soon as all disagreement miniECG recordings are assessed by a third cardiologist. However, because gold standard reference 12-lead ECG was often not available in this study, this might still limit the interpretation of study results.

For the 12-lead ECG, elaborate guidelines exist for the interpretation of the ECG[62–67]. In ***Chapter 5***, such criteria were developed for miniECG recordings. MiniECG recordings of patients with confirmed normal SR show little variation in P-wave polarity and T-wave polarity and therefore a draft definition of normal SR could be developed for the miniECG. While polarity of waves is important, especially in assessment of rhythm and ischemia in the ECG, criteria on amplitudes of waves, morphology of waves, conduction times, frequency and regularity have yet to be researched. Not only should this be done to define normal SR on the miniECG, sensitive and specific criteria have yet to be developed for miniECG abnormalities.

It is not yet known how much the positioning of the miniECG varies between and within users, as well as the effect this has on the recordings. Findings described in ***Chapter 5*** regarding difficulty of determining the QRS-axis, might indicate variance in and influence of different measuring positions. It is important to further investigate whether this plays a role, because changes to the miniECG design and or app should then be made, to improve consequent positioning.

The study described in ***Chapter 5,*** ultimately aims to acquire a set of data large enough to evaluate the vast majority of ECG abnormalities. However, with datasets of the expected size of >14,000 ECGs, the analysis presented in ***Chapter 5*** is not feasible. Algorithms for the automated analysis of ECGs exist, which automatically and with high precision calculate ECG parameters. The miniECG research group has worked on a median beat algorithm as the first step in the evaluation and comparison of ECGs. Once this algorithm is validated, it can be used to obtain median beats of all study ECGs and to calculate the correlation between different ECGs. This allows more precise comparison of the two, both quantitative and qualitative. When delineation of the ECG is added to the algorithm, parameters of the miniECG and 12-lead ECG recordings can be compared and thresholds for abnormalities can then be established.

Continuous development of the miniECG

This research line not only focusses on the (pre-)clinical validation of the miniECG, the miniECG itself has been improved along the studies. Using the feedback of the end-users (both research team and healthcare professionals), several adjustments were made to the miniECG 1.0, eventually resulting in a miniECG 1.1. In clinical practice, healthcare workers often forgot to turn-off the device after recording a miniECG. This is why the on-off button of the miniECG 1.0 was substituted with a push button together with a sleep mode function, where the device automatically enters sleep mode and can be woken up through the push button. In addition, several changes were made to the miniECG app to be more intuitive and to minimize the number of steps needed to perform a measurement.

Inability of live-viewing of the miniECG was identified as a major factor in low quality miniECG recordings in clinical studies. Under set-circumstances, high quality miniECG were recorded sequentially by researchers of the miniECG, for example in the pre-clinical study as described in ***Chapter 3***. However, in clinical settings as described in ***Chapter 4*** and ***Chapter 5***, miniECG recordings of insufficient quality were often obtained (+-20%). Reasons for this were hard to pinpoint, as measurements were performed by a large team of healthcare professionals at relatively low frequency. Some factors were identified that generally improve the quality of recordings. These include the application of ECG contact spray, avoiding movement of the miniECG device at the start and during recording, removing any electrical devices to minimize 50Hz noise and instructing the patient not to move. Water tightness of the device was improved to minimize the risks of leaking of contact spray into the device, causing unpredictable errors in recording.

Nonetheless, additional instruction of the healthcare professionals executing the recordings did not result in >90% sufficient quality miniECGs. This is why development was focused towards showing live miniECG. A new app version and new firmware were developed to be able to view leads II and M3. These leads use all four electrodes of the miniECG and thereby give insight into contact of all electrodes and occurrence of noise. 10 seconds of live miniECG can be viewed. When pressing the record button, the last 10-seconds of the live miniECG are saved as the miniECG recording, thereby optimizing both quality of the recording and reducing the amount of time needed to acquire a recording.

Another factor hindering the efficiency of clinical studies was the limited battery life of the miniECG. While batteries can easily be replaced, this hinders clinical workflow and thereby has a large effect on the practical feasibility of miniECG clinical studies. For this reason, a latch-circuit was integrated into the design of the miniECG enabling reduction of energy usage much more than any sleep-mode would allow. With the

latch-circuit, the miniECG allows for >30days of stand-by mode and >300 recordings, well beyond the requirements for the current clinical studies.

Planned improvements include improving versatility of the miniECG app, specifically the development of dedicated apps for different end-users. For a patient at home, it is cumbersome to fill in a personal ID with each individual recording, while in professional healthcare settings this is crucial. Other optimizations for specific users include the input of symptoms, room to make notes for researchers and options for rapid sequential recordings and increasing the sampling frequency of the miniECG from 250Hz to 500Hz which is standard in clinical ECG.

Future of the miniECG

Added value of a self-use mobile ECG device is limited as long as experienced cardiologists are needed for the interpretation of the ECG. On top of this, interpretation of different lead settings requires niche expertise. A way to overcome these challenges is to incorporate automated algorithms into the miniECG software. An example of such an algorithm is a deep learning algorithm for triage of 12-lead ECGs by van de Leur et al[73]. This algorithm triages 12-lead ECGs into normal, abnormal non-acute, abnormal sub-acute, and acute with high discrimination across all categories[73]. Other possibilities would be to apply machine learning to compare sequential miniECGs and detect differences.

Studies have suggested that machine learning algorithms can reach similar performance on fewer lead ECG[74]. If it would be possible to translate the miniECG into an ECG that is similar to a 12-lead ECG, this would largely increase options in the application of available 12-lead ECG interpretation algorithms for miniECG recordings. Deep-neural networks have been applied to identify underlying factors of variation of the ECG. Van de Leur et al. have shown that the 12-lead ECG can be encoded into 21 continuous factors of variation[75]. If similar methods can be used to translate the miniECG into factors of variation, this could be used to 'reconstruct' a 12-lead ECG from the miniECG.

High sensitivity in the detection of STEMI is essential, as rapid intervention is needed to minimize morbidity and mortality of the disease, ischemic ST-deviation varies highly in different stages of myocardial infarction. A slightly lower sensitivity of the miniECG in late myocardial ischemia might be accepted, as the miniECG can be used to acquire ECG earlier compared to 12-lead ECG and recording of the ECG can be easily repeated, both improving sensitivity in situations more similar to the intended use of the miniECG. If more elaborate research into the sensitivity of the miniECG reveals a low sensitivity, this might be compensated

for by additional measuring protocols. An additional measurement with the miniECG positioned at the apex or at the left midaxillary line might increase sensitivity in the detection of ischemia. Or a personalized position may be beneficial to optimize for highest ECG voltages. The ultimate challenge remains to facilitate rapid and easy recording of an ECG by a patient, even in times of physical or emotional stress. The value of additional steps should therefore always be critically evaluated.

To work more towards the intended use of the miniECG, studies should focus on self-use by patients. This will bring new challenges, regarding usability of the device. Especially measuring quality may largely decrease. As seen in the studies presented in this thesis, measuring quality varied largely. For this reason live visualization was developed. While healthcare professionals can adequately estimate signal quality based on visual inspection, automated algorithms are needed to guide patients in the acquisition of high-quality signal.

References

1. Holst, H., Ohlsson, M., *et al.* A confident decision support system for interpreting electrocardiograms. *Clinical Physiology* **19**, 410–418 (1999).
2. Wood, G., Batt, J., *et al.* Exploring the impact of expertise, clinical history, and visual search on electrocardiogram interpretation. *Medical Decision Making* **34**, 75–83 (2014).
3. Brady, W. & Alibertis, Kostas. *The ECG for prehospital emergency care*. (Wiley Blackwell, 2013).
4. Ibanez, B., James, S., *et al.* 2017 ESC Guidelines for the management of acute myocardial infarction in patients presenting with ST-segment elevation. *European Heart Journal* vol. 39 119–177 (2018).
5. Foo, C. Y., Bonsu, K. O., *et al.* Coronary intervention door-to-balloon time and outcomes in ST-elevation myocardial infarction: A meta-analysis. *Heart* **104**, 1362–1369 (2018).
6. Terkelsen, C. J., Sørensen, J. T., *et al.* System delay and mortality among patients with STEMI treated with primary percutaneous coronary intervention. *JAMA - Journal of the American Medical Association* **304**, 763–771 (2010).
7. Diercks, D. B., Kontos, M. C., *et al.* Utilization and Impact of Pre-Hospital Electrocardiograms for Patients With Acute ST-Segment Elevation Myocardial Infarction. Data From the NCDR (National Cardiovascular Data Registry) ACTION (Acute Coronary Treatment and Intervention Outcomes Network) Re. *J Am Coll Cardiol* **53**, 161–166 (2009).
8. Collet, J.-P., Thiele, H., *et al.* 2020 ESC Guidelines for the management of acute coronary syndromes in patients presenting without persistent ST-segment elevation. *European Heart Journal* **42**, 1289–1367 (2020).
9. Rutten, F. H., Kessels, A. G. H., *et al.* Electrocardiography in primary care; is it useful? *International Journal of Cardiology* **74**, 199–205 (2000).
10. Chan, L., Willemsen, R., *et al.* Elektrocardiografie in de huisartsenpraktijk. *Tijdschrift voor praktijkondersteuning* **9**, 118–122 (2014).
11. Schläpfer, J. & Wellens, H. J. Computer-Interpreted Electrocardiograms: Benefits and Limitations. *J Am Coll Cardiol* **70**, 1183–1192 (2017).
12. Cook, D. A., Oh, S. Y., *et al.* Accuracy of Physicians' Electrocardiogram Interpretations: A Systematic Review and Meta-analysis. *JAMA Intern Med* **180**, 1461–1471 (2020).

13. Salerno, S. M., Alguire, P. C., *et al.* Competency in interpretation of 12-lead electrocardiograms: a summary and appraisal of published evidence. *Ann Intern Med* **138**, 751–760 (2003).

14. Holmvang, L., Hasbak, P., *et al.* Differences between local investigator and core laboratory interpretation of the admission electrocardiogram in patients with unstable angina pectoris or non-Q-wave myocardial infarction (a thrombin inhibition in myocardial ischemia [TRIM] substudy). *American Journal of Cardiology* **82**, 54–60 (1998).

15. Bogun, F., Anh, D., *et al.* Misdiagnosis of atrial fibrillation and its clinical consequences. *American Journal of Medicine* **117**, 636–642 (2004).

16. Southern, W. N. & Arnsten, J. H. The effect of erroneous computer interpretation of ECGs on resident decision making. *Medical Decision Making* **29**, 372–376 (2009).

17. Morganroth, J. & Gussak, I. ECG Acquisition and Signal Processing. in *Cardiac Safety of Noncardiac Drugs: Practical Guidelines for Clinical Research and Drug Development* (eds. Morganroth, J. & Gussak, I.) 131–46 (Humana Press, 2005). doi:10.1007/978-1-59259-884-7.

18. Wilson, F. N., Johnston, F. D., *et al.* The precordial electrocardiogram. *American Heart Journal* **27**, 19–85 (1944).

19. Freeman, D. K., Gatzke, R. D., *et al.* Saturation of the right-leg drive amplifier in low-voltage ECG monitors. *IEEE Trans Biomed Eng* **62**, 323–330 (2015).

20. Wilson, F. N., Johnston, F. D., *et al.* Electrocardiograms that represent the potential variations of a single electrode. *American Heart Journal* **9**, 447–458 (1934).

21. Caillol, T., Strik, M., *et al.* Accuracy of a Smartwatch-Derived ECG for Diagnosing Bradyarrhythmias, Tachyarrhythmias, and Cardiac Ischemia. *Circ Arrhythm Electrophysiol* **14**, 102–104 (2021).

22. Bansal, A. & Joshi, R. Portable out-of-hospital electrocardiography: A review of current technologies. *Journal of Arrhythmia* **34**, 129–138 (2018).

23. National Academy of Sciences. *Guide for the Care and Use of Laboratory Animals*. (WA, USA: The National Academies Pres, 2011).

24. Lim, H. C. S., Salandanan, E. A., *et al.* Inter-rater reliability of J-point location and measurement of the magnitude of ST segment elevation at the J-point on ECGs of STEMI patients by emergency department doctors. *Emerg Med J* **32**, 809–812 (2015).

25. Okada, J. I., Fujiu, K., *et al.* Ionic mechanisms of ST segment elevation in electrocardiogram during acute myocardial infarction. *Journal of Physiological Sciences* **70**, (2020).

26. Kleber, A. G. Resting Membrane Potential, Extracellular Potassium Activity, and Intracellular Sodium Activity during Acute Global Ischemia in Isolated Perfused Guinea Pig Hearts. *Circulation Research* **52**, 442–450 (1983).

27. Wiegerinck, R. F., Glvez-Monton, C., *et al.* Changes in QRS duration and R-wave amplitude in electrocardiogram leads with ST segment elevation differentiate epicardial and transmural myocardial injury. *Heart Rhythm* **7**, 1667–1673 (2010).

28. Shenasa, M., Hamel, D., *et al.* Body Surface Potential Mapping of ST-segment Shift in Patients Undergoing Percutaneous Transluminal Coronary Angioplasty Correlations With the ECG and Vectorcardiogram. *Journal of Electrocardiology* **26**, 43–51 (1993).

29. Nedios, S., Romero, I., *et al.* Precordial electrode placement for optimal ECG monitoring: Implications for ambulatory monitor devices and event recorders ☆. *Journal of Electrocardiology* (2014) doi:10.1016/j.jelectrocard.2014.04.003.

30. Figueras A'*, J. & Bermejo, B. Additional elevation of the ST segment: a possible early electrocardiographic marker of experimental myocardial reperfusion. *Gwdiovascular Research Cmdiovascul~ Research* **32**, 1141–1147 (1996).

31. Kleinbongard, P., Amanakis, G., *et al.* Reflection of cardioprotection by remote ischemic perconditioning in attenuated ST-segment elevation during ongoing coronary occlusion in pigs evidence for cardioprotection from ischemic injury. *Circulation Research* **122**, 1102–1108 (2018).

32. Diego, J. M. di & Antzelevitch, C. Ischemic Ventricular Arrhythmias Experimental Models and Their Clinical Relevance. *Heart Rhythm* **8**, 1963 (2011).

33. Terkelsen, C. J. The reperfusion ST-peak in acute myocardial infarction. *Journal of Electrocardiology* **44**, 82–83 (2011).

34. Simonis, G., Strasser, R. H., *et al.* Reperfusion injury in acute myocardial infarction. *Critical Care* **16**, A22 (2012).

35. Wehrens, X. H. T., Doevendans, P. A., *et al.* A comparison of electrocardiographic changes during reperfusion of acute myocardial infarction by thrombolysis or percutaneous transluminal coronary angioplasty. *Am Heart J* **139**, 430–436 (2000).

36. Doevendans, P. A., Gorgels, A. P., *et al.* Electrocardiographic diagnosis of reperfusion during thrombolytic therapy in acute myocardial infarction. *Am J Cardiol* **75**, 1206–1210 (1995).

37. Schreiber, W., Kittler, H., *et al.* Additional ST-segment elevation during thrombolytic therapy in patients with acute ST-elevation myocardial infarction: impact on myocardial salvage and final infarct size. *Wien Klin Wochenschr* **115**, 104–110 (2003).

38. Demidova, M. M., van der Pals, J., *et al.* ST-segment dynamics during reperfusion period and the size of myocardial injury in experimental myocardial infarction. *Journal of Electrocardiology* **44**, 74–81 (2011).

39. Rumeau, P., Fourcade, J., *et al.* ST-segment changes after direct current external cardioversion for atrial fibrillation. Incidence, characteristics and predictive factors. *International Journal of Cardiology* **148**, 341–346 (2011).

40. Ben-Dov, I. Z., Leibowitz, D., *et al.* ST-segment elevation post cardioversion: A current of injury without injury. *International Journal of Cardiology* **106**, 255–256 (2006).

41. Cantor, A., Stein, B., *et al.* "Intermittent" and transient ST-segment elevation following direct current cardioversion. *International Journal of Cardiology* **20**, 403–405 (1988).

42. van Gelder, I. C., Crijns, H. J., *et al.* Incidence and clinical significance of ST segment elevation after electrical cardioversion of atrial fibrillation and atrial flutter. *American Heart Journal* **121**, 51–56 (1991).

43. Clauss, S., Bleyer, C., *et al.* Animal models of arrhythmia: classic electrophysiology to genetically modified large animals. *Nature Reviews Cardiology 2019 16:8* **16**, 457–475 (2019).

44. Crick, S. J., Sheppard, M. N., *et al.* Anatomy of the pig heart : comparisons with normal human cardiac structure. *Journal of Anatomy* **193**, 105–119 (1998).

45. Moser, D. K., Kimble, L. P., *et al.* Reducing delay in seeking treatment by patients with acute coronary syndrome and stroke: A scientific statement from the American Heart Association Council on Cardiovascular Nursing and Stroke Council. *Circulation* **114**, 168–182 (2006).

46. Nallamothu, B., Normand, S., *et al.* Relation between door-to-balloon times and mortality after primary percutaneous coronary intervention over time: a retrospective study. *The Lancet* **385**, 1114–1122 (2015).

47. Squire, B. T., Tamayo-Sarver, J. H., *et al.* Effect of prehospital cardiac catheterization lab activation on door-to-balloon time, mortality, and false-positive activation. *Prehospital Emergency Care* **18**, 1–8 (2014).

48. Stowens, J. C., Sonnad, S. S., *et al.* Using EMS dispatch to trigger STEMI alerts decreases door-to-balloon times. *West J Emerency Medicine* **16**, 472–480 (2015).

49. Fordyce, C. B., Al-Khalidi, H. R., *et al.* Association of Rapid Care Process Implementation on Reperfusion Times Across Multiple ST-Segment-Elevation Myocardial Infarction Networks. *Circulation: Cardiovascular Interventions* **10**, (2017).

50. Gräsner, J.-T., Herlitz, J., *et al.* European Resuscitation Council Guidelines 2021: Epidemiology of cardiac arrest in Europe. *Resuscitation* **161**, 61–79 (2021).

51. Carnlöf, C., Schenck-Gustafsson, K., *et al.* Instant electrocardiogram feedback with a new digital technique reduces symptoms caused by palpitations and increases health-related quality of life (the RedHeart study). *Eur J Cardiovasc Nurs* **20**, 402–410 (2021).

52. Khan, M. A., Hashim, M. J., *et al.* Global Epidemiology of Ischemic Heart Disease: Results from the Global Burden of Disease Study. *Cureus* **12**, (2020).

53. Thygesen, K., Alpert, J. S., *et al.* Third universal definition of myocardial infarction. *Circulation* **126**, 2020–2035 (2012).

54. Riley, R. F., Newby, L. K., *et al.* Diagnostic time course, treatment, and in-hospital outcomes for patients with ST-segment elevation myocardial infarction presenting with nondiagnostic initial electrocardiogram: a report from the American Heart Association Mission: Lifeline program. *Am Heart J* **165**, 50–56 (2013).

55. Taher, T., Fu, Y., *et al.* Aborted myocardial infarction in patients with ST-segment elevation: insights from the Assessment of the Safety and Efficacy of a New Thrombolytic Regimen-3 Trial Electrocardiographic Substudy. *J Am Coll Cardiol* **44**, 38–43 (2004).

56. Verheugt, F. W. A., Gersh, B. J., *et al.* Aborted myocardial infarction: a new target for reperfusion therapy. *European Heart Journal* **27**, 901–904 (2006).

57. Riley, R. F. & McCabe, J. M. ST-segment elevation myocardial infarction: Challenges in diagnosis. *US Cardiology Review* **10**, 91–94 (2016).

58. Members, W. C., Antman, E. M., *et al.* ACC/AHA Guidelines for the Management of Patients With ST-Elevation Myocardial Infarction—Executive Summary. *Circulation* **110**, 588–636 (2004).

59. Johnson, D. M., Junarta, J., *et al.* Usefulness of Mobile Electrocardiographic Devices to Reduce Urgent Healthcare Visits. *Am J Cardiol* **153**, 125–128 (2021).

60. van Heuverswyn, F., de Buyzere, M., *et al.* Feasibility and performance of a device for automatic self-detection of symptomatic acute coronary artery occlusion in outpatients with coronary artery disease: a multicentre observational study. *The Lancet Digital Health* **1**, e90–e99 (2019).

61. Hayashi, M., Shimizu, W., *et al.* The Spectrum of Epidemiology Underlying Sudden Cardiac Death. *Circulation Research* **116**, 1887–1906 (2015).

62. Surawicz, B., Childers, R., *et al.* AHA/ACCF/HRS recommendations for the standardization and interpretation of the electrocardiogram: Part III: Intraventricular conduction disturbances: A scientific statement from the American Heart Association Electrocardiography and Arrhythmias Committee, Council on Clinical Cardiology; The American College of Cardiology Foundation; And the Heart Rhythm Society. *Circulation* **119**, (2009).

63. Mason, J. W., Hancock, E. W., *et al.* Recommendations for the standardization and interpretation of the electrocardiogram: Part II: Electrocardiography diagnostic statement list: A scientific statement from the American Heart Association Electrocardiography and Arrhythmias Committee, Council on Clinical Cardiology; the American College of Cardiology Foundation; and the Heart Rhythm Society. *Circulation* **115**, 1325–1332 (2007).

64. Kligfield, P., Gettes, L. S., *et al.* Recommendations for the standardization and interpretation of the electrocardiogram: Part I: The electrocardiogram and its technology: A scientific statement from the American Heart Association Electrocardiography and Arrhythmias Committee, Council on Clinical Cardiology; the American College of Cardiology Foundation; and the Heart Rhythm Society. *Circulation* **115**, 1306–1324 (2007).

65. Hancock, E. W., Deal, B. J., *et al.* AHA/ACCF/HRS Recommendations for the Standardization and Interpretation of the Electrocardiogram: Part V: Electrocardiogram Changes Associated With Cardiac Chamber Hypertrophy A Scientific Statement From the American Heart Association Electrocardiography and Arrhythmias Committee, Council on Clinical Cardiology; the American College of Cardiology Foundation; and the Heart Rhythm Society Endorsed by the International Society for Computerized Electrocardiology. *J Am Coll Cardiol* **53**, 992–1002 (2009).

66. Rautaharju, P. M., Surawicz, B., *et al.* AHA/ACCF/HRS Recommendations for the Standardization and Interpretation of the Electrocardiogram. Part IV: The ST Segment, T and U Waves, and the QT Interval A Scientific Statement From the American Heart Association Electrocardiography and

Arrhythmias Committee, Council on Clinical Cardiology; the American College of Cardiology Foundation; and the Heart Rhythm Society. *J Am Coll Cardiol* **53**, 982–991 (2009).

67. Wagner, G. S., Macfarlane, P., *et al.* AHA/ACCF/HRS Recommendations for the Standardization and Interpretation of the Electrocardiogram. Part VI: Acute Ischemia/Infarction A Scientific Statement From the American Heart Association Electrocardiography and Arrhythmias Committee, Council on Clinical Cardiology; the American College of Cardiology Foundation. *J Am Coll Cardiol* **53**, 1003–1011 (2009).

68. Sadanaga, T., Sadanaga, F., *et al.* An evaluation of ECG leads used to assess QT prolongation. *Cardiology* **105**, 149–154 (2006).

69. Salvi, V., Karnad, D. R., *et al.* Choice of an alternative lead for QT interval measurement in serial ECGs when Lead II is not suitable for analysis. *Indian Heart Journal* **64**, 535 (2012).

70. Vandenberk, B., Vandael, E., *et al.* Which QT Correction Formulae to Use for QT Monitoring? *Journal of the American Heart Association: Cardiovascular and Cerebrovascular Disease* **5**, (2016).

71. Kenny, B. J. & Brown, K. N. ECG T Wave. *StatPearls* (2022).

72. Willems, J. L., Zywietz, C., *et al.* Influence of noise on wave boundary recognition by ECG measurement programs. Recommendations for preprocessing. *Computers and Biomedical Research* **20**, 543–562 (1987).

73. van de Leur, R. R., Blom, L. J., *et al.* Automatic Triage of 12-Lead ECGs Using Deep Convolutional Neural Networks. *J Am Heart Assoc* **9**, e015138 (2020).

74. Galloway, C. D., Valys, A. V., *et al.* Development and Validation of a Deep-Learning Model to Screen for Hyperkalemia from the Electrocardiogram. *JAMA Cardiology* **4**, 428–436 (2019).

75. Leur, R. R. van de, Bos, M. N., *et al.* Inherently explainable deep neural network-based interpretation of electrocardiograms using variational auto-encoders. *medRxiv* 2022.01.04.22268759 (2022) doi:10.1101/2022.01.04.22268759.

76. MAC VU360 | GE Healthcare (United States). https://www.gehealthcare.com/products/diagnostic-ecg/resting-ecg/mac-vu360.

Supplements

Supplement S3.1: Timing of miniECG recordings

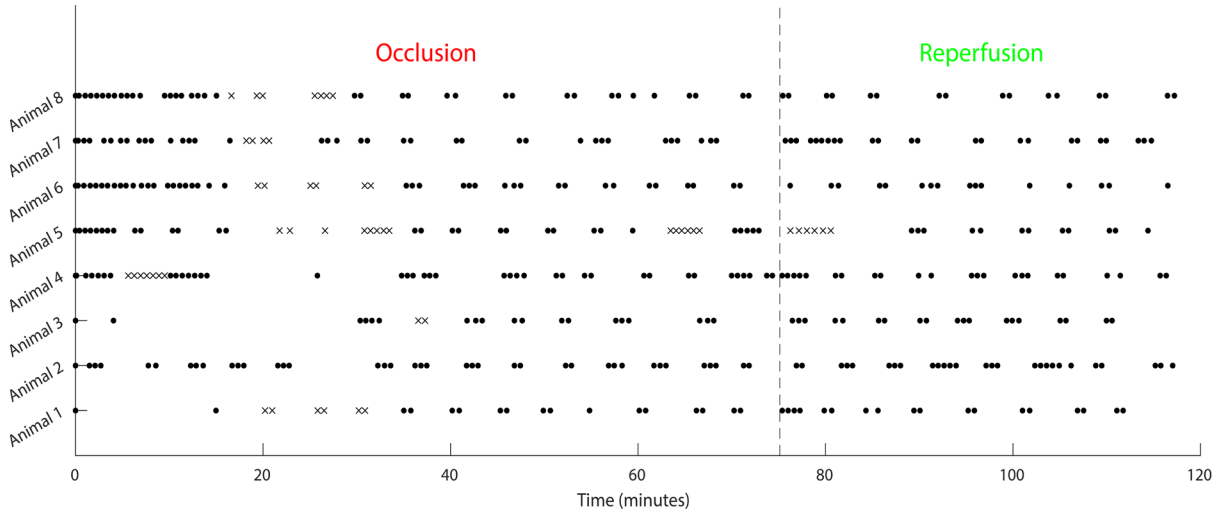

Figure S3.1: Timing of miniECG recordings for all eight animals separately. Each dot represents one recording. Datapoints marked 'x' correspond to measurements excluded from trendlines and further analysis, due to a defibrillation shock being administered in the 5 minutes prior to the measurement.

Supplement S3.2: ST-deviation in individual animals

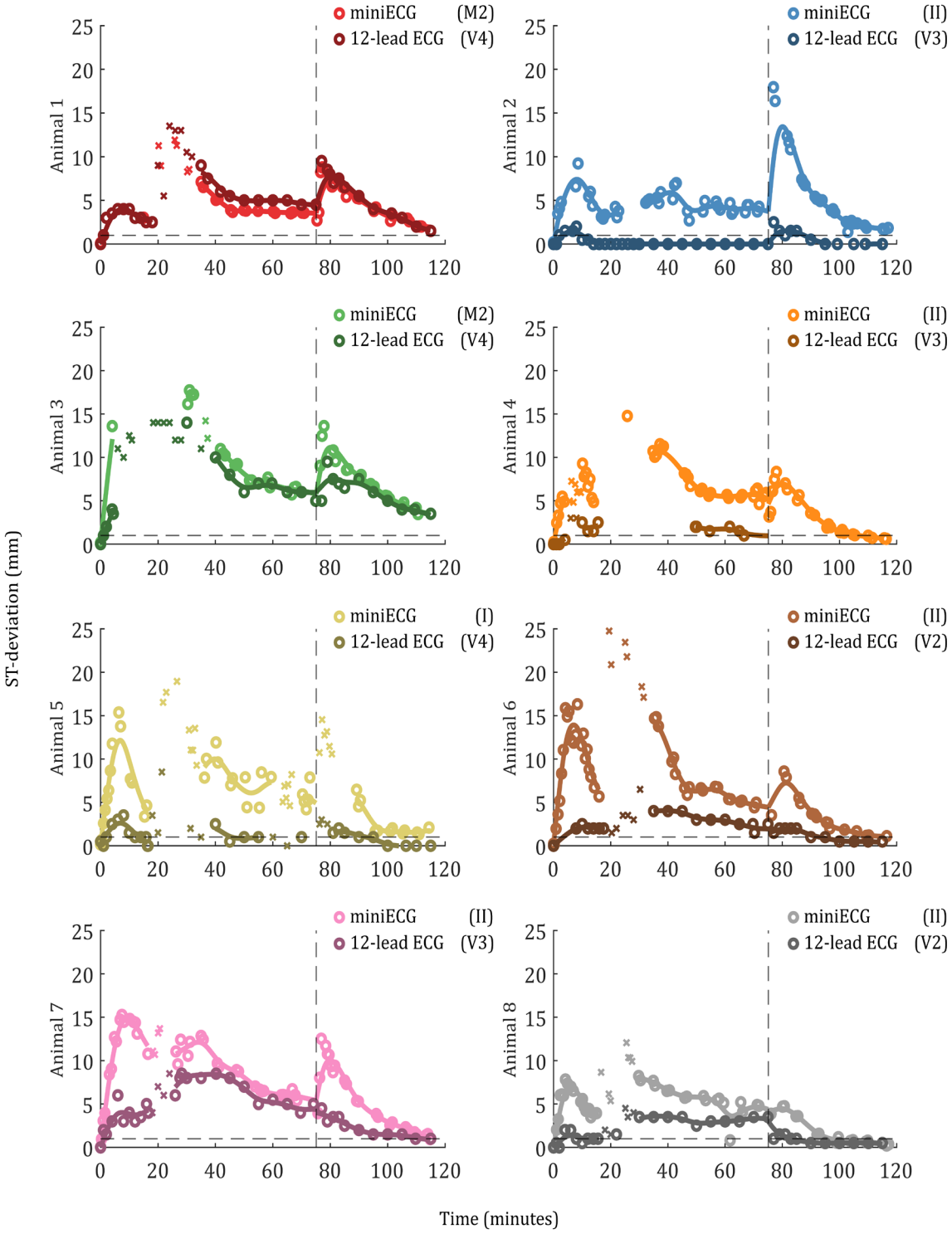

Figure S3.2: ST-deviation in leads showing maximal deviation. A comparison between miniECG and 12-lead ECG per animal. Identified maximal ST-deviation leads are shown in the legends. Reperfusion at 75 minutes is indicated with vertical dashed lines. Datapoints marked 'x' correspond to measurements excluded from trendlines and further analysis, due to a defibrillation shock being administered in the 5 minutes prior to these measurements.

Supplement S3.3: ST-deviation corrected for baseline QRS-amplitude

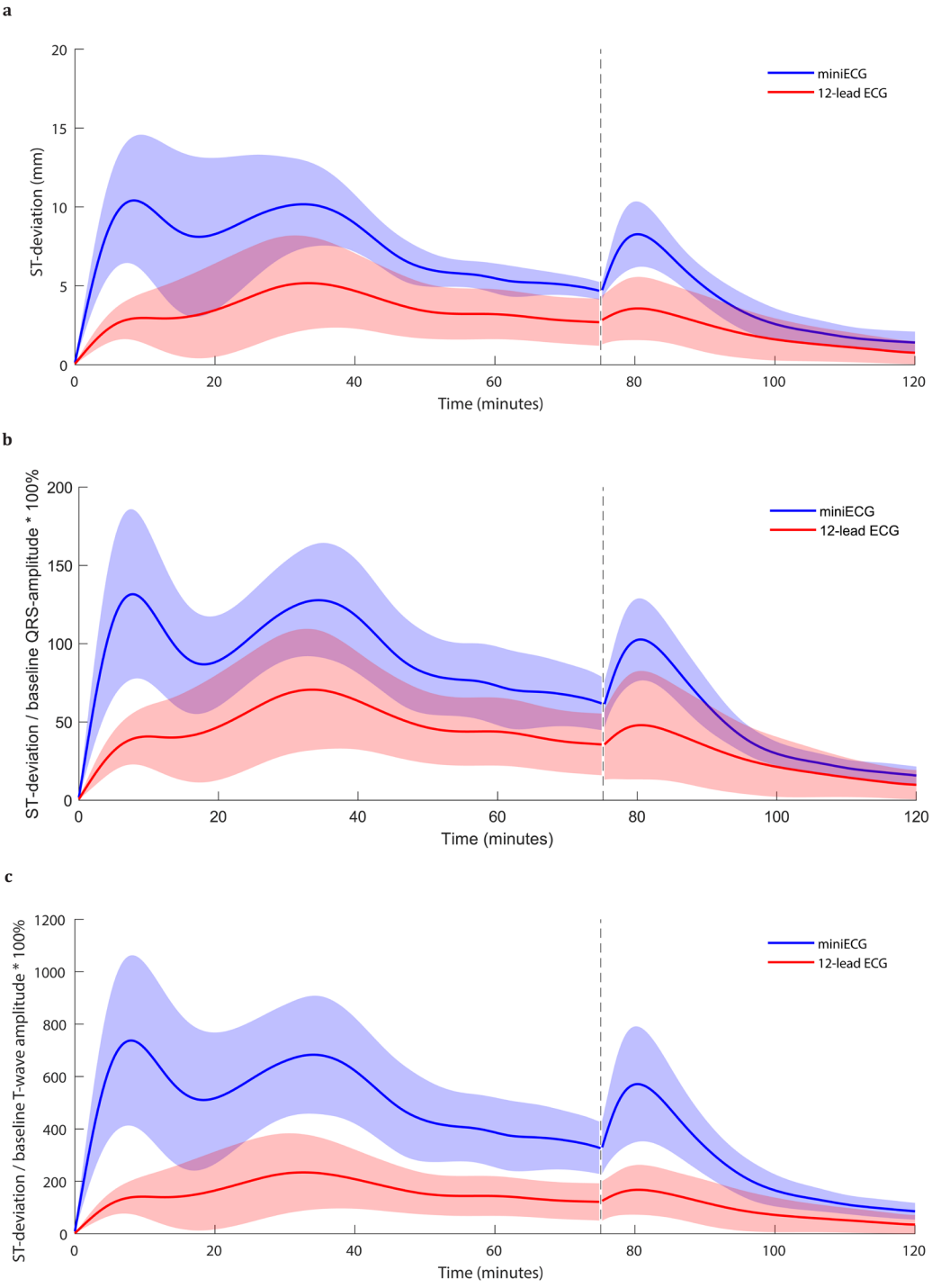

Figure S3.3: a. Mean ST-deviation and 95%CI of the most deviated leads of the miniECG and 12-lead ECG during the occlusion period and reperfusion period. b. ST-deviation corrected for baseline QRS-amplitude. c. ST-deviation corrected for baseline T-wave amplitude.

Supplement S5.1: Incidence of ECG abnormalities in the UMCU

Category	ECG abnormality	Number of ECGs with this label since 2017 (%)	Expected number of inclusions*
Conduction disorders	First degree AV block	18.57	2592
Conduction disorders	Second degree AV block	0.53	74
Conduction disorders	Third degree AV block	0.38	53
Conduction disorders	Left bundle branch block	11.44	1597
Conduction disorders	Right bundle branch block	25.14	3510
Conduction disorders	Bifascicular or trifascicular block	4.04	564
Conduction disorders	Aspecific intraventricular conduction delay	11.27	1574
Conduction disorders	Aberration	5.63	786
Rhythm disorders	Sinus arrythmia	15.30	2136
Rhythm disorders	Sinus tachycardia	25.30	3533
Rhythm disorders	Sinus bradycardia	29.75	4154
Rhythm disorders	Atrial rhythm	2.29	320
Rhythm disorders	Atrial fibrillation	16.47	2300
Rhythm disorders	Atrial flutter	5.03	702
Rhythm disorders	Premature atrial complex	16.10	2247
Rhythm disorders	Premature ventricular complex	19.57	2732
Rhythm disorders	Supraventricular tachycardia	1.52	213
Rhythm disorders	Ventricular tachycardia	0.17	24
Rhythm disorders	Narrow complex tachycardia	0.19	26
Rhythm disorders	Broad complex tachycardia	3.22	449
Rhythm disorders	Junctional or ventricular escape rhythm	3.61	504
Rhythm disorders	AV(N)RT	0.21	30
Rhythm disorders	WPW pattern	0.21	30
Ischemia	Acute ischemia anterior	1.87	261
Ischemia	Acute ischemia inferior	4.05	565
Ischemia	Acute ischemia lateral	1.80	252
Ischemia	Acute ischemia posterior	0.40	56
Ischemia	Old ischemia anterior	20.10	2806
Ischemia	Old ischemia inferior	23.91	3338
Ischemia	Old ischemia lateral	7.23	1009
Ischemia	Old ischemia posterior	1.32	184
Other	Left ventricular hypertrophy	17.02	2376
Other	Right ventricular hypertrophy	2.57	358
Other	Atrial enlargement	12.48	1743
Other	Negative T-wave	1.02	142
Other	Aspecific ST-segment or T-wave abnormalities	56.12	7836
Other	Early repolarization	1.32	184
Other	Long QT-syndrome	12.54	1751
Other	Pericarditis	0.62	86
Other	Abnormal r-wave progression	2.54	355
Other	Pacemaker spikes	14.10	1969

Table S5.1: Incidence of ECG abnormalities in the UMC Utrecht database containing all 12-lead ECGs from 2017 onwards. *The number of inclusions is depicted based on a sample size of 13962 patients

Acknowledgements

This thesis marks the end of my time as a Technical Medicine student. I would like to express my appreciation to the people who've helped me along the way.

I want to thank everyone involved in the miniECG project for giving me the opportunity to work in this dynamic and innovation driven environment. Thank you for your direct feedback during bi-weekly meetings and for sharing your expertise. René van Es and Rutger van der Leur, your versatility is inspiring. Your enthusiasm and never-ending drive have motivated me throughout this year. Thank you for the countless research discussions from which I've learned a lot. Alejandra Zepeda-Echavarria, you have always been eager to try out new ideas and we teamed up many times on side projects. Thank you for your great science tips and on how to cook 'Tinga de pollo'. Niek Ratering-Arntz, your relaxed and open attitude have made it easy to approach challenges and to work on solutions. Rutger Hassink, you've supported my clinical goals and helped me position myself the clinic. Thank you for your practical tips and feedback.

My supervisors from the University of Twente have guided and supported me during my internships. Elyse Walter and Paul van Katwijk, you have motivated me to challenge myself and to advocate my opinions. Kees Slump, you always find a way to give new perspectives on subjects, even outside of your research expertise. Thank you for your inspiring words.

Dear members of bRAXIS, 'het leukste clubje van Enschede', I do not know where to start or where to end. I want to thank you for all the adventures and I hope there are more to come. Lotte Hazeleger, Quinten Eyck, Justin te Wildt, together we've started this adventure. We all know that without you, 19-year-old me would never have coped with the confusing logistics of being a first-year bachelor student. Thank you for your open mindsets and humor.

Dear parents, your perseverance and conscientious working attitude have shaped me into who I am. Thank you for always listening and for your unconditional support.

Nynke de Vries

April 13th, 2022